APPENDICE I: manuale di CORMIX III

CORMIX3: AN EXPERT SYSTEM FOR MIXING ZONE ANALYSIS AND PREDICTION OF BUOYANT SURFACE DISCHARGES

by

Gilbert R. Jones, Jonathan D. Nash and Gerhard H. Jirka

DeFrees Hydraulics Laboratory

School of Civil and Environmental Engineering

Cornell University

Ithaca, New York 14853-3501

Cooperative Agreement No. CR 818527

Project Officer:

Dr. Hiranmay Biswas

OFFICE OF SCIENCE AND TECHNOLOGY

U.S. ENVIRONMENTAL PROTECTION AGENCY

WASHINGTON, DC 20460

Chapter I
CORMIX3 - An Expert System for Mixing Zone Analysis and Prediction of Buoyant Surface Discharges

1.1 Scope and Objectives

The **Cor**nell **Mi**xing Zone E**x**pert System - Subsystem **3**, (CORMIX3) is a knowledge-based engineering tool which utilizes a flow classification scheme that assures that the appropriate modelling technique is applied to each of the variety of flows that may result. In this manner, CORMIX3 may be used to analyze a majority of positively and neutrally buoyant surface discharges with a high degree of accuracy.

CORMIX3 is the third of a series of subsystems which make up the CORMIX Expert System. The first subsystem, CORMIX1, was developed for the prediction and analysis of submerged single port discharges (Doneker and Jirka, 1990). The second subsystem, CORMIX2, was subsequently developed for submerged multiport diffusers (Akar and Jirka, 1991). These systems have been distributed since 1990 from Cornell University and as public-domain models form the USEPA Center for Environmental Assessment Modeling, Athens, Georgia, since 1990. While the first two systems were originally distributed as stand-alone applications, CORMIX Versions 2.0 and higher, distributed since 1993, are an integrated package containing all three subsystems with flexible switching among these different design solutions.

As an expert system, CORMIX3 is a user-friendly program which guides the user through the analysis of a particular discharge configuration. To facilitate its use, ample instructions are provided, suggestions for improving dilution characteristics are included, and warning messages are displayed when undesirable or uncommon flow conditions occur. In addition, a graphical interface is included to give the user a "visual picture" of the flow. Finally, and most important, the system should provide accurate predictions of the trajectory, dilution and geometry of the flow.

1.2 History of Length-scale Models

This section provides a history of the mathematical technique used in this study to predict the important quantitative characteristics of buoyant surface jets. It is divided into three subsections. Section 1.2.1 explains the three basic groups of mathematical models for buoyant surface jet analysis. Section 1.2.2 reviews the history of the simple analytical expressions used to describe submerged round buoyant jets. Section 1.2.3 discusses various attempts to apply these simple analytical expressions to buoyant surface jets and suggests how models based on similar analyses may be developed for buoyant surface jet problems.

1.2.1 Description of Three General Model Types

The several types of mathematical models which have been developed for submerged round buoyant jets may be grouped into the following categories: jet-integral models, three-dimensional numerical models, and "length-scale" models. Jet-integral models are described by Jirka et al. (1981) as follows:

"Jet-integral models consist of a set of ordinary differential equations derived from the cross-sectional (normal to the jet trajectory) integration of jet-properties such as mass,

momentum, and buoyancy fluxes. Empirical formulations for internal jet behavior such as buoyant damping of turbulence and cross-sectional distortion (lateral spreading) are included. The equation systems are parabolic and are solved by simple forward-marching numerical schemes along the jet trajectory."

Jet-integral models perform satisfactorily for simple flows with no shoreline interaction or attachment. However, strong crosscurrents or limited depths causing attachment with the downstream bank or strong initial buoyancy causing intrusion of the effluent along the upstream bank render these models invalid. In addition, jet-integral models predict only the jet-like behavior of the flow near the source. They are incapable of simulating any far-field processes that occur after a certain transition distance (Jirka et al., 1981).

Three-dimensional numerical models attempt to approximate the system of Reynolds equations through finite element or finite difference schemes. To a large extent, these methods have been unsuccessful for routine engineering applications. Jirka et al. (1975) summarizes the difficulties with numerical models as follows:

"The major problem seems to be the specification of boundary conditions, in addition, the formulation of turbulent transport terms is unknown... . From a practical viewpoint the models are highly complicated, difficult to check, have no instructions for the user and are expensive to use (even in moderate size test cases)."

The third class of modeling techniques, called herein "length-scale models," provides the basic methodology utilized in this study. Surface discharge flows can be divided up into different regimes each dominated by particular flow properties such as the initial momentum, the buoyancy flux, or the ambient crossflow. Within each regime, the flow may be approximated with simple asymptotic relationships derived from basic equations describing the simplified problem for which only the most significant properties are accounted for, and then adding perturbation terms to account for lesser effects. The models that use these asymptotic solutions are referred to as "length-scale" models because of the use of specific length scales to delineate the extent of the regimes for which these analytical expressions are valid.

The following subsections discuss the historical development of the asymptotic solutions used to describe the flow regimes of buoyant flows. Initially, analytical expressions and length scales were developed for submerged round buoyant jets. However, they have subsequently been extended to buoyant surface jet analysis.

1.1.2 Review of Submerged Round Buoyant Jet Expressions

Most of the earlier work leading up to our present length-scale models originated from studies of smokestack plumes which grew out of the increasing need for air pollution control. Early studies, such as those by Schmidt (1941), Yih (1951), Rouse, Yih, and Humphreys (1952), Railston (1954), Priestley and Ball (1955), Morton, Taylor, and Turner (1956), and Slawson and Csanady (1967), focused on pure plumes for which the initial momentum of the discharge can be considered negligible. Much of this work pointed to a height-width relationship of $b \propto z$ and a trajectory relationship of plumes in a crossflow of $z \propto x^{2/3}$, where b is the plume half-width, z is the vertical height of the plume centerline, and x is the horizontal coordinate downwind.

Scorer (1958, 1959) recognized the potential importance of an initial momentum regime. Scorer (1959) concluded that a buoyant jet has three regimes dominated by momentum, buoyancy, and passive advection successively. Using simple physical arguments and dimensional analysis he determined that the trajectory relationships for a buoyant jet were $z \propto x^{1/3}$ for the momentum dominated regime and $z \propto x^{2/3}$ for the buoyancy dominated regime. Similarly, he concluded that $b \propto z$ for both of these near-field regimes. Scorer's idea

of the two distinguishable regimes in the near-field received little attention for nearly a decade.

Csanady (1961) was the first to introduce length scales into buoyant jet analysis. He used a plume-to-crossflow length scale, Lb* = Jo*/ua3, where Jo* = uo(do/2)2go' and uo is the effluent exit velocity, do is the diameter of the discharge outlet, and go' is the reduced gravitational acceleration. Note, this definition of a plume-to-crossflow length scale differs from the definition used in the remainder this study by a factor of 21/2, i.e.: Lb = 21/2Lb*. Previously, Morton (1959) had non-dimensionalized his results with the flux ratio Mo3/4/Jo1/2, where Mo is the initial momentum flux and Jo is the initial buoyancy flux. This term would later be dubbed a momentum-buoyancy length scale, however Morton never recognized it as a significant independent term. Csanady reasoned through dimensional analysis that the trajectory of a buoyant jet had the functional form of:

$$\frac{z}{L_b} = f\left(\frac{x}{L_b}, Fr_o, \frac{d_o}{L_b}\right) \tag{1.1}$$

where Fro is the discharge Froude number defined as:

$$Fr_o = \frac{u_o}{\sqrt{g_o' d_o}} \tag{1.2}$$

At sufficiently large values of z/Lb, the influence of Fro and do/Lb becomes negligible, resulting in the following simplified relationship:

$$\frac{z}{L_b} = f\left(\frac{x}{L_b}\right) \tag{1.3}$$

Csanady also noted that this was an asymptotic formula and that "the effective origin of z may have to be moved to allow for a 'momentum rise'." He compared Eqn. 1.3 with the asymptotic forms of the equations derived by Priestley (1956) and Sutton (1953) which suggested that (z/Lb) ∝ (x/Lb)3/4 and (z/Lb) ∝ (x/Lb)2/3 respectively and found both fit observed results reasonably well considering the scatter of data.

Csanady's study was followed up by both Briggs (1965) and Moore (1966). Briggs used a plume-to-crossflow length scale in equations obtained through dimensional analysis to describe pure plumes in a crossflow. He concluded the rise due to buoyancy without the effect of ambient stratification was governed by the relationship:

$$\frac{z}{L_b} = 2.0\left(\frac{x}{L_b}\right)^{\frac{2}{3}} \tag{1.4}$$

He determined the terminal height of the plume was also a function of the plume-to-crossflow length scale. In addition, Briggs gave relationships that were determined in the same manner for stratified ambient conditions which were not of the form of Eqn. 1.3. Moore, on the other hand, used a plume-to-crossflow length scale in relationships developed from the conservation equations. He also obtained trajectory results in the form of Eqn. 1.3 for continuous plumes.

Hoult, Fay, and Forney (1969) were the first to use a jet-to-crossflow length scale and to develop simple formulae for the momentum dominated regime. They used the jet-to-crossflow length scale, $Lm^* = (do/2)(uo/ua)$ where ua is the ambient flow velocity, and the plume-to-crossflow length scale, Lb, in asymptotic relationships developed from conservation and entrainment equations. Note that this definition of the jet-to-crossflow length scale differs from the jet-to-crossflow length scale used in the remainder of this study by a factor of $\pi 1/2$, i.e.: $Lm = \pi 1/2 Lm^*$. They recognized three near-field flow regimes of a buoyant jet, two which were governed by the relationships:

$$\frac{z}{L_m} = K_1 \left(\frac{x}{L_m} \right)^{\frac{1}{2}} \quad ; \quad z << L_m \tag{1.5}$$

$$\frac{z}{L_b} = K_2 \left(\frac{x}{L_b} \right)^{\frac{2}{3}} \quad ; \quad z >> L_b \ \& \ L_m \tag{1.6}$$

They contested that "no simple formula exists" for the intermediate regime where $Lm < z < Lb$. The constants K1 and K2 are dependent on the entrainment coefficients which were determined experimentally. Subsequent work by Fay (1973) attempted to extrapolate Hoult, Fay, and Forney's analysis to stratified ambient environments and to motor vehicles and aircraft wakes.

Chu and Goldberg (1974) attempted to link the momentum dominated and buoyancy dominated regimes into one relationship by using an alternate entrainment hypothesis, claiming that "the transition between the two regimes cannot be derived from dimensional analysis." Their proposed relationships for the transition were:

$$\frac{z}{L_b} = C_1 \left\{ \frac{1}{2} \left(\frac{x}{L_b} \right)^2 + \left(\frac{L_m}{L_b} \right)^2 \left(\frac{x}{L_b} \right) \right\}^{\frac{1}{3}} \tag{1,7}$$

$$\frac{b}{L_b} = C_2 \left\{ \frac{1}{2} \left(\frac{x}{L_b} \right)^2 + \left(\frac{L_m}{L_b} \right)^2 \left(\frac{x}{L_b} \right) \right\}^{\frac{1}{3}} \tag{1.8}$$

$$S = C_3 \left(\frac{u_o}{u_a} \right) \left\{ \frac{1}{2} \left(\frac{L_b}{L_m} \right) \left(\frac{x}{L_m} \right)^2 + \left(\frac{x}{L_m} \right) \right\}^{\frac{1}{3}} \tag{1.9}$$

where S is the dilution along the plume centerline, defined as C/Co, C being the centerline pollutant concentration anywhere along the trajectory and Co the initial pollutant concentration at the discharge. Note that the trajectory relationship reduces to Eqns. 1.5 and

1.6 for their respective regimes of dominance. Chu and Goldberg were able to show a decent fit to experimental data with these relationships.

An extension of Hoult, Fay, and Forney's work was carried out by Hoult and Weil (1972). Using the same method as Hoult, Fay, and Forney but a different entrainment hypothesis, they were able to determine the following relationships for the three different regimes:

weakly deflected jet

$$\frac{z}{L_m} = K_1 \left(\frac{x}{L_m} \right)^{\frac{1}{2}} \quad ; \quad z << L_m \tag{1.10}$$

strongly deflected plume

$$\frac{z}{L_b} = K_2 \left(\frac{x}{L_b} \right)^{\frac{2}{3}} \quad ; \quad x >> L_m \;\&\; L_b \tag{1.11}$$

strongly deflected jet

$$\frac{z}{L_b} = K_3 \left(\frac{x}{L_m} \right)^{\frac{1}{3}} \quad ; \quad z >> L_m \tag{1.12}$$

K1, K2, and K3 are constants which were determined experimentally. Hoult and Weil obtained the relationship for the strongly deflected jet region by taking the asymptotic result for a non-buoyant discharge for large values of x/Lb. Note Hoult and Weil assume that Lm<Lb, thereby neglecting the possibility of a weakly deflected plume regime that might exist in the intermediate region.

Hoult and Weil also determined transition criteria for the different regimes. For a pure jet, they concluded that the transition criteria from the weakly deflected jet region to the strongly deflected jet region occurs at x ∝ Lm, the transition from the weakly deflected jet region to the strongly deflected plume region occurs at x ∝ Lm3/Lb2, and if the intermediate strongly deflected jet regime exists, then the transition from the weakly deflected jet region to the strongly deflected jet region occurs at x ∝ Lm2/Lb.

Wright (1977) generalized Hoult and Weil's length-scale model using dimensional analysis in a comprehensive study on vertical buoyant jets in a crossflow. Wright used four length scales: the jet-to-crossflow length scale, Lm, the plume-to-crossflow length scale, Lb, a discharge length scale, LQ = Qo/Mo1/2, and a jet-to-plume length scale, LM = Mo3/4/Jo1/2. Wright proposed that any jet property, Æ, can be described as a function of three length scale ratios:

$$\phi = f\left(\frac{z}{L_m}, \frac{L_b}{L_m}, \frac{L_Q}{L_m} \right) \tag{1.13}$$

LM is not present in Eqn. 1.13 since it is a combination of Lm and Lb such that LM = (Lm3/Lb)1/2. Using simple physical arguments and dimensional considerations he obtained solutions for the different flow regimes for a vertical buoyant jet in a crossflow as shown in

Table 1.1. The dilution equations were obtained using the assumption of similarity between velocity and concentration profiles, a condition that has proven accurate in many previous studies for all but the strongly deflected plume regime. He supported the use of these asymptotic equations and found values for the constants C1 - C8 by comparing them with both his own data and experiments run by Fan (1967). Table 1.2 shows the sequence of regimes determined by the length-scale ratio Lm/Lb.

Since the publication of Wright's paper, investigators have attempted to extend these simple formulae and length scales to other buoyant jet scenarios. One such study conducted by Bühler and Hauenstein (1979) extended Wrights analysis to buoyant jets discharged horizontally perpendicular to the crossflow. Making certain analogies to Wright's trajectory relationships and using simple physical arguments they obtained the relationships for 3-dimensional trajectories and dilutions. The results of their study revealed that the horizontal trajectory (i.e.: the trajectory seen in a plan view) is a function of one parameter, Lm/Lb, and the independent variable, x/Lm:

$$\frac{y}{L_M} = f\left(\frac{x}{L_M}, \frac{L_m}{L_b}\right) \tag{1.14}$$

Bühler and Hauenstein also used a similar analysis to describe buoyant jets discharged into stagnant ambient environments.

More recent work by Knudsen (1988) extended Wright's (1977) work to include horizontal jets in a still ambient, co-flow, crossflow, and counterflow. However, Knudsen used an excess momentum flux, Me = (π/4)do_uo(uo-ua), where uo and ua are vector quantities. The use of the excess momentum flux instead of the absolute momentum flux was proposed earlier by List and Imberger (1973).

The use of these length-scale models have proven successful in predicting the bulk characteristics of smokestack plumes, sewer outfalls, and similar round buoyant jet scenarios. Fischer et al. (1979) gives a comprehensive review of turbulent jets and plumes and the application of length-scale analysis to these problems. Length-scale analysis have since been extended to submerged discharges in stratified environments (Doneker and Jirka, 1990), multiport diffuser problems (Akar and Jirka, 1990), and buoyant surface jets (Chu and Jirka, 1986). The following subsection discusses the use of length-scale models for buoyant surface jets.

1.2.3 Applying Length-scale Models to Surface Buoyant Jets

Attempts to extend length-scale models to buoyant surface jets have also been made, although their use in this capacity has not been studied as extensively as for submerged round jets. One of

Tab 1: Wright's (1977) Trajectory and Dilution Relationships for a Submerged Buoyant Jet Discharged Vertically in a Crossflow

Flow Regime	Trajectory	Dilution
Weakly deflected jet	$\frac{z}{L_m} = C_1 \left(\frac{x}{L_m}\right)^{\frac{1}{2}}$	$S\frac{Q_o u_a}{M_o} = C_5 \left(\frac{x}{L_m}\right)$
strongly deflected jet	$\frac{z}{L_m} = C_2 \left(\frac{x}{L_m}\right)^{\frac{1}{3}}$	$S\frac{Q_o u_a}{M_o} = C_6 \left(\frac{x}{L_m}\right)^{2}$
weakly deflected plume	$\frac{z}{L_b} = C_3 \left(\frac{x}{L_b}\right)^{\frac{3}{4}}$	$g'\frac{J_o}{u_a^5} = C_7 \left(\frac{x}{L_b}\right)^{-5/3}$
strongly deflected plume	$\frac{z}{L_b} = C_4 \left(\frac{x}{L_b}\right)^{\frac{2}{3}}$	$g'\frac{J_o}{u_a^5} = C_8 \left(\frac{x}{L_b}\right)^{-2}$

Tab 1.2: Sequence of Flow Regimes as Defined by Wright (1977) for Submerged Buoyant Jets

$\frac{L_m}{L_b} >> 1$	momentum dominated:	weakly deflected jet ® strongly deflected jet ® strongly deflected plume
$\frac{L_m}{L_b} << 1$	buoyancy dominated:	weakly deflected jet ® weakly deflected plume ® strongly deflected plume
$\frac{L_m}{L_b} \approx 1$	small middle region:	weakly deflected jet &PEГ; strongly deflected plume

Tab 1.3; Bühler and Hauenstein's (1979) Trajectory Relationships

Flow Regime	y-Trajectory	z-Trajectory
Weakly deflected jet	$\frac{y}{L_m} = C_9 \left(\frac{x}{L_m}\right)^{\frac{1}{2}}$	$\frac{z}{L_m} = C_{13} \left(\frac{L_m^{1/2}}{L_M^{2/3}} x^{3/2}\right)^{1/2}$
strongly deflected jet	$\frac{y}{L_m} = C_{10} \left(\frac{x}{L_m}\right)^{\frac{1}{3}}$	$\frac{z}{L_m} = C_{14} \left(\frac{L_b^{5/9}}{L_M^{2/3}} x^{3/2}\right)^{1/2}$
weakly deflected plume	$\frac{y}{L_M} = C_{11}$	$\frac{z}{L_b} = C_{15} \left(\frac{x}{L_b}\right)^{3/4}$
strongly deflected plume	$\frac{y}{L_M} = C_{12}$	$\frac{z}{L_b} = C_{16} \left(\frac{x}{L_b}\right)^{2/3}$

Tab 1.4: Bühler and Hauenstein's (1979) Dilution Relationships

Flow Regime	Dilution
Weakly deflected jet	$S = C_{17} \left(\frac{L_M^2}{L_Q^3} z\right)^{1/3}$
strongly deflected jet	$S = C_{18} \left(\frac{L_M^{4/3}}{L_Q^2 L_b^{1/3}} z\right)^{1/2}$
weakly deflected plume	$S = C_{19} \left(\frac{1}{L_Q^3 L_M^2} z^5\right)^{1/3}$
strongly deflected plume	$S = C_{20} \left(\frac{1}{L_Q L_m} z^2\right)$

the first applications of length-scale models to buoyant surface jets was proposed by Jirka et al. (1981). They compared trajectory data of free surface jets to the weakly deflected jet and strongly deflected jet regimes of a submerged jet and found similar power laws but with deviations corresponding to the product of the initial densimetric Froude number and the

inverse of the velocity ratio, R, which is defined as uo/ua. They suggest that for the weakly deflected region of the surface jet, the trajectory has the relation:

$$\frac{y}{L_m} = C_1 \left(\frac{x}{L_m} \right)^{\frac{1}{2}} \tag{1.15}$$

while in the strongly deflected regime, the relationship is:

$$\frac{y}{L_M} = C_2 \left(\frac{x}{L_m} \right)^{\frac{1}{3}} \tag{1.16}$$

The constants of proportionality, C1 and C2, are dependent on the quantity Fro/R.

Different scaling laws have been proposed by Abdelwahed and Chu (1981). The relationships use a concept of a line impulse which makes this approach more applicable to strongly bent over flows where the current is the primary advecting mechanism and the lateral penetration into the flow is included as a perturbation.

Length scales have also been used to determine empirical expressions describing upstream intruding plumes (Jones et al., 1985) and the extent of recirculation of shoreline attached jets (Chu and Abdelwahed, 1990). However, a comprehensive study of length-scale model applications to buoyant surface jets has not been made. Due to the differences between surface buoyant jets and submerged jets, care must be taken when applying such length-scale analysis as originally proposed by Wright to surface buoyant jets. However, since fundamental similarities exist and some applicability has been recognized, it is reasonable to expect that by developing simple analytical expressions to describe their relative regimes of dominance, practical predictions can be made of the flow behavior in most buoyant surface jet scenarios.

Chapter II
Theoretical Background

The analysis of buoyant surface jets can be simplified by recognizing two separate regions: the "near-field" and the "far-field" (see Figure 2.1). The near-field designates the extent of the flow near the discharge in which the mixing is highly dependent on the discharge conditions, whereas the mixing in the far-field is dependent solely on the ambient conditions.

The dilution in the near-field is highly dependent on the initial volume, momentum, and buoyancy flux of the discharge. Different discharge configurations can lead to fundamentally different flow characteristics in the near-field. This forms the basis for classifying buoyant surface jets. Four categories of near-field flow patterns can be distinguished: free jets, wall jets, shoreline attached flows, and upstream intruding plumes. These four major flow categories are qualitatively described in Section 2.1.

In the far-field, ambient turbulence, stratification, wind shear, and many other factors dependent on the ambient conditions play a role in determining the rate of mixing. Lateral spreading due to buoyancy and passive diffusion caused by ambient turbulence are the predominant flow processes in a majority of practical situations. Since most other processes are difficult to model and/or are generally insignificant, only buoyant spreading and passive diffusion will be considered in the far-field.

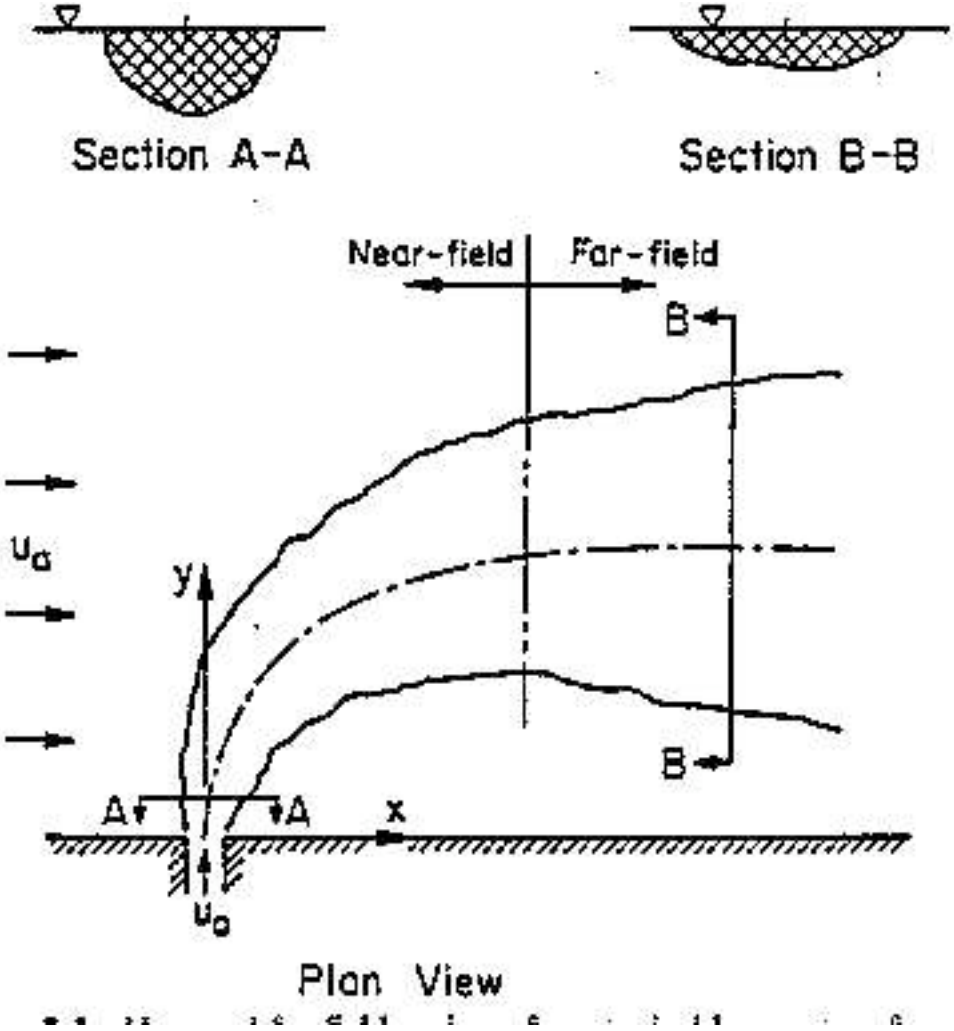

Fig 2.1: Near and far-field regimes for a typical bouyant surface jet.

It is apparent that no clear transition from the near-field to the far-field exists for buoyant surface jets. Although the transition is gradual, an approximate point of transition can be estimated by using particular length scales. Length scales can be used to delineate regimes within the flow in which particular mixing processes dominate. These length scales are described in Section 2.2.

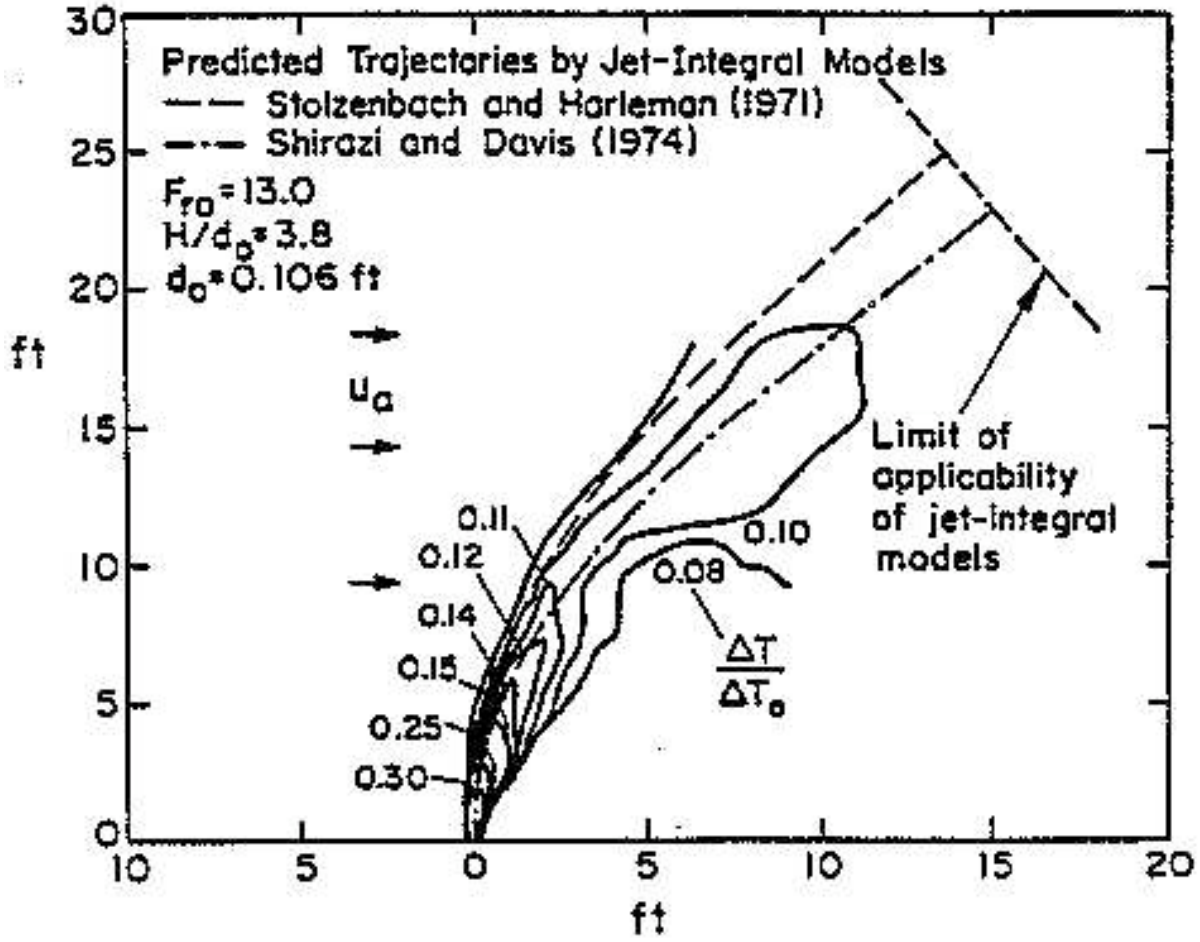

Fig 2.2: Surface Isotherms of a bouyant surface jat. (From Koester, 1974).

Section 2.3 and 2.4 describe the theoretical considerations and development of the near-field and far-field regimes respectively. The near-field region includes various flow regimes that make up free jets, wall jets, shoreline attached jets, and upstream intruding plumes. The far-field includes the two processes of buoyant spreading and passive diffusion.

2.1 General Description of Flow Patterns

The distinction of four major flow categories is based on observations in the field and laboratory. Three of the four near-field flow patterns (free jets, shoreline attached jets, and upstream intruding plumes) were first quantitatively defined by Chu and Jirka (1986). The fourth, wall jets, are special cases of free jets and will be discussed along with free jets in Section 2.1.1. The following discussion describes each of these patterns and the processes that are involved.

2.1.1 Free Jets and Wall Jets

Free jets are characterized by a gradual bending so that the flow does not interact with the near shoreline. Figure 2.2 shows the surface isotherms of a typical free jet produced by a heated water discharge. Chu and Jirka (1986) have described the crossflow as having two effects on a free jet. The first is to entrain ambient momentum into the jet causing a gradual "bending" of the jet, and the second is to discourage unsteady buoyant spreading by advecting the plume-like spreading downstream.

Free-jets can be divided into two regimes analogous to submerged jets: a weakly deflected regime and a strongly deflected regime. The weakly deflected regime is characterized by strong initial jet-like mixing which is slightly advected downstream. Within this regime, there may be a transition from this strong jet-like mixing to a buoyancy-induced spreading mechanism, however the trajectory is still similar to that of a weakly deflected submerged jet dictated by the initial momentum. The theoretical development for the weakly deflected region is discussed in Section 2.3.3.1.

In the strongly deflected regime, the flow is advected downstream with the ambient current, but still retains some horizontal momentum which carries it further outward into the ambient flow. In this regime, jet mixing or buoyant spreading mechanisms may dominate. The trajectory remains similar to that of a strongly deflected submerged jet. The strongly deflected regime ends where its lateral progression becomes negligible and far-field processes take over. The theoretical development for the strongly deflected region is discussed in Section 2.3.3.2.

In stagnant ambient environments, only the weakly deflected regime exists. Figure 2.3 demonstrates a typical buoyant surface jet into a stagnant environment. At the end of the weakly deflected regime, a pool of buoyant effluent is established which spreads laterally unsteadily in all directions. The flow near the discharge is characterized by a constantly increasing depth representing the jet-like mixing, while further from the source a decrease in the plume depth occurs where buoyancy-induced spreading takes over. The transition distance in Figure 2.3 represents the end of the weakly deflected regime and the beginning of the unsteady buoyant spreading. The development of the mathematical relationships for buoyant surface jets discharged into stagnant environments is described in Section 2.3.2.

Bottom interaction may occur in free jets. However, if bottom interaction occurs too close to the discharge, it may block off the ambient flow, forcing the jet against the near bank causing shoreline attachment. If bottom interaction does occur without causing shoreline attachment, both the weakly deflected regime and the strongly deflected regime can exist, but will not be dominated by buoyant spreading since buoyant spreading results in detachment from the bottom and restratification of the plume.

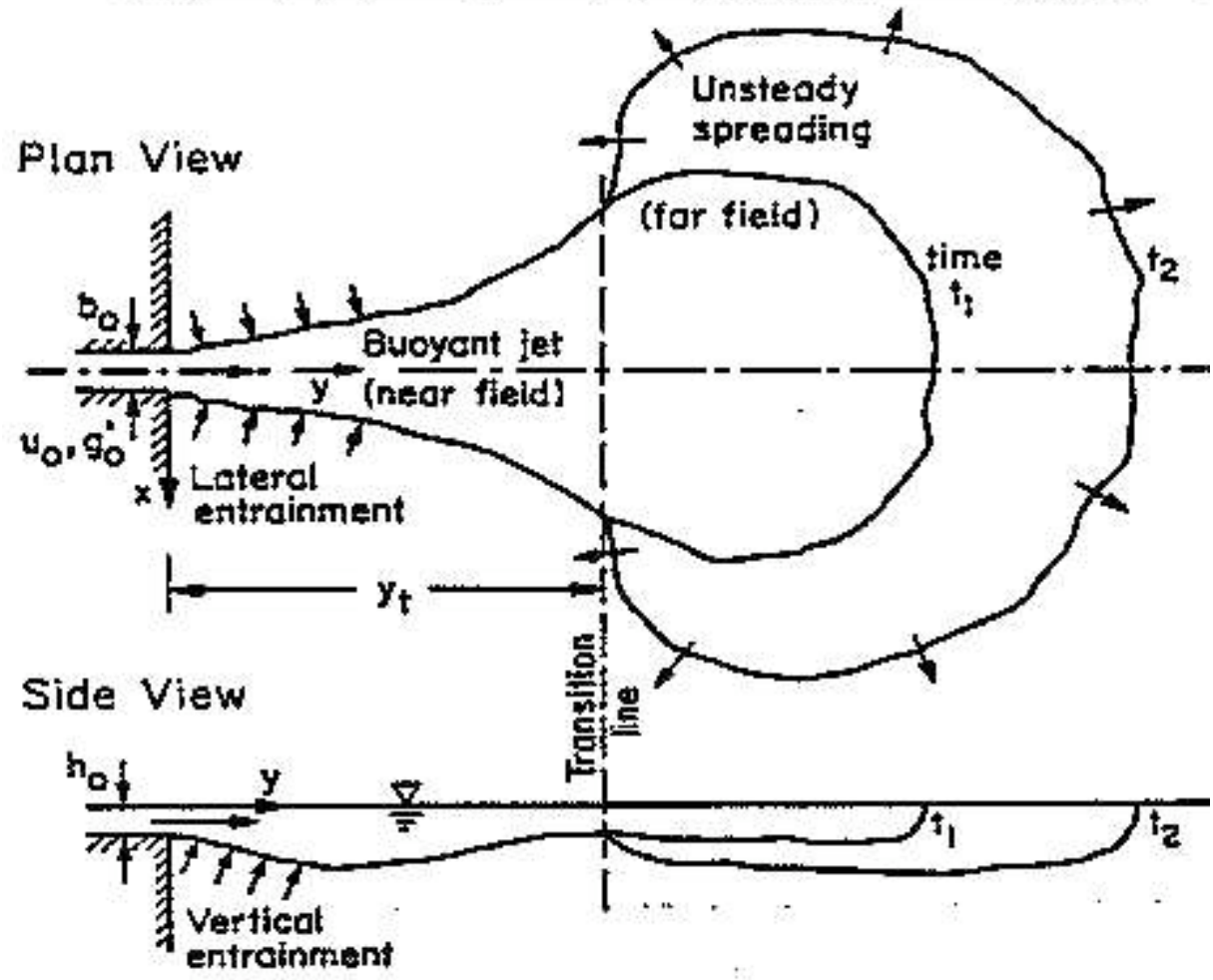

Fig 2.3: Typical bouyant surface jat in a stagnant environment.

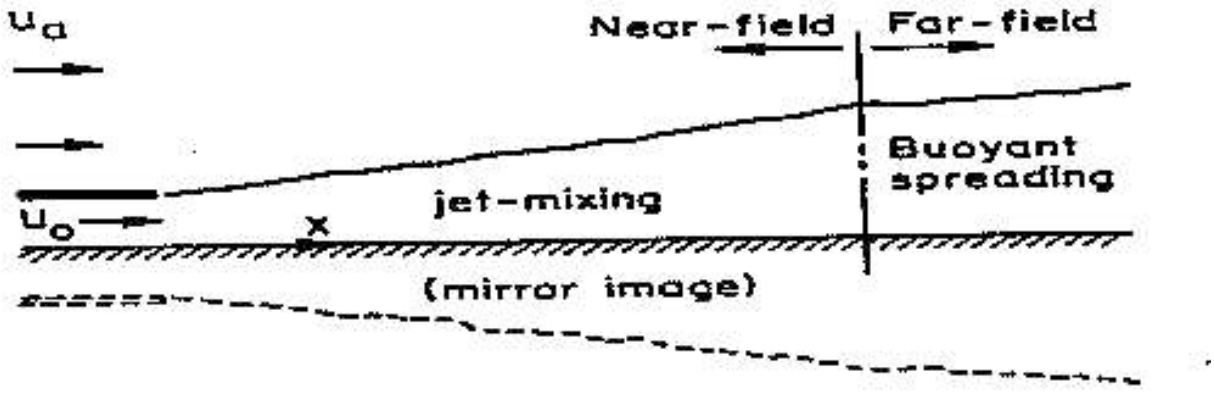

Fig 2.4: Typical wall jet. The mirror image likends the flow to a surface jet in a coflow.

Wall jets can be considered weakly deflected jets which are discharged in a coflow along the bank(see Figure 2.4). The bank then acts as a reflective boundary along which a mirror image can be created. As with free jets, the initial mixing within the weakly deflected regime is jet-like. However, at the transition to the far-field, this jet-mixing becomes secondary, and buoyant spreading and/or passive diffusion becomes dominant. The theoretical development for wall jets is discussed in Section 2.3.4.

2.1.2 Shoreline Attached Jets

There are two phenomenon that cause dynamic attachment of the flow to the downstream shoreline. First, a strong crosscurrent can bend the jet over far enough to cause it to dynamically attach to the bank. Second, discharging over the whole depth of the receiving water can effectively "block off" the ambient current causing the flow to be pushed against the downstream shoreline. Characteristic of shoreline attached jets is the recirculation of effluent along the downstream bank caused by the wake effects in the lee of the jet. This is illustrated in Figure 2.5.

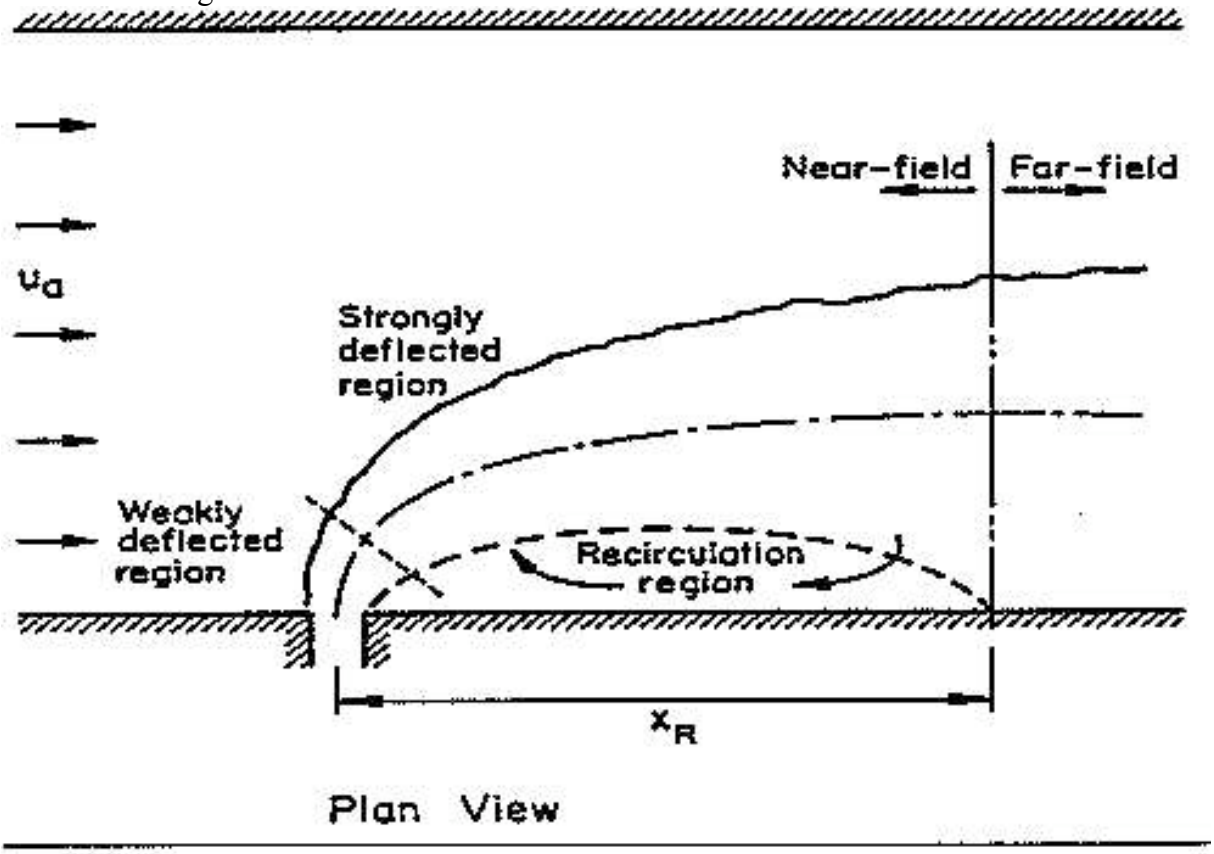

Fig 2.5: Schematic of a shoreline attached flow.

Shoreline attachment reduces the lateral progression of the jet. However, similar flow regimes to those found in free jets can be recognized: weakly deflected shoreline attached jet regime and strongly deflected shoreline attached jet/plume regime. It is unlikely that in the weakly deflected shoreline attached regime buoyancy will dominate since it is usually very short in extent due to the extreme initial bending. However, in the strongly deflected regime, buoyancy may take over producing buoyancy-induced lateral spreading. This will occur only in situations with no bottom attachment. The mathematical relationships for these regimes are developed in Section 2.3.5.

2.1.3 Upstream Intruding Plumes

In cases where strongly buoyant effluent is discharged into a slowly moving environment, upstream intrusion may develop. In upstream intruding plumes, a front is formed where the buoyant upstream intrusion is balanced by the shearing force at the head of the plume. The distance the plume intrudes along the upstream bank is denoted by the symbol x_s. (see Figure 2.6a). The near-field is limited to the area of the plume upstream of the discharge and a short distance downstream. At a distance x_s downstream from the discharge, the plume exhibits the far-field processes of buoyant spreading and then passive diffusion.

If the depth at the discharge is shallow and the effluent is discharged with sufficiently high momentum and buoyancy, the flow may be unstable and full vertical mixing with recirculation may occur in the immediate vicinity of the discharge. This is illustrated in Figure 2.6b. Restratification generally occurs just downstream of the point of discharge where far-field processes take over.

2.2 Length Scales

Length scales measure the relative importance of the initial volume flux, momentum flux, buoyancy flux, and crossflow velocity. Four length scales have practical meaning for use in buoyant surface jets analysis: the discharge length scale, jet-to-plume length scale, jet-to-crossflow length scale, and plume-to-crossflow length scale. Two dimensional definitions of the first three length scales are also used for situations where there is bottom interaction and the flow can be considered two dimensional. Each of these length scales are described in detail in the following subsections.

2.2.1. Discharge Length Scale

The discharge length scale measures the relative significance of the volume flux as compared to the momentum flux, and is defined as:

$$L_Q = \frac{Q_o}{M_o^{1/2}} \tag{2.1}$$

The discharge length scale defines the region for which discharge channel geometry strongly influences the flow characteristics. This comprises the zone of flow establishment, and is generally insignificant in extent. Note that this length scale plays a critical role when measured against the jet-to plume length scale (discussed below) in determining whether upstream intrusion occurs or not.

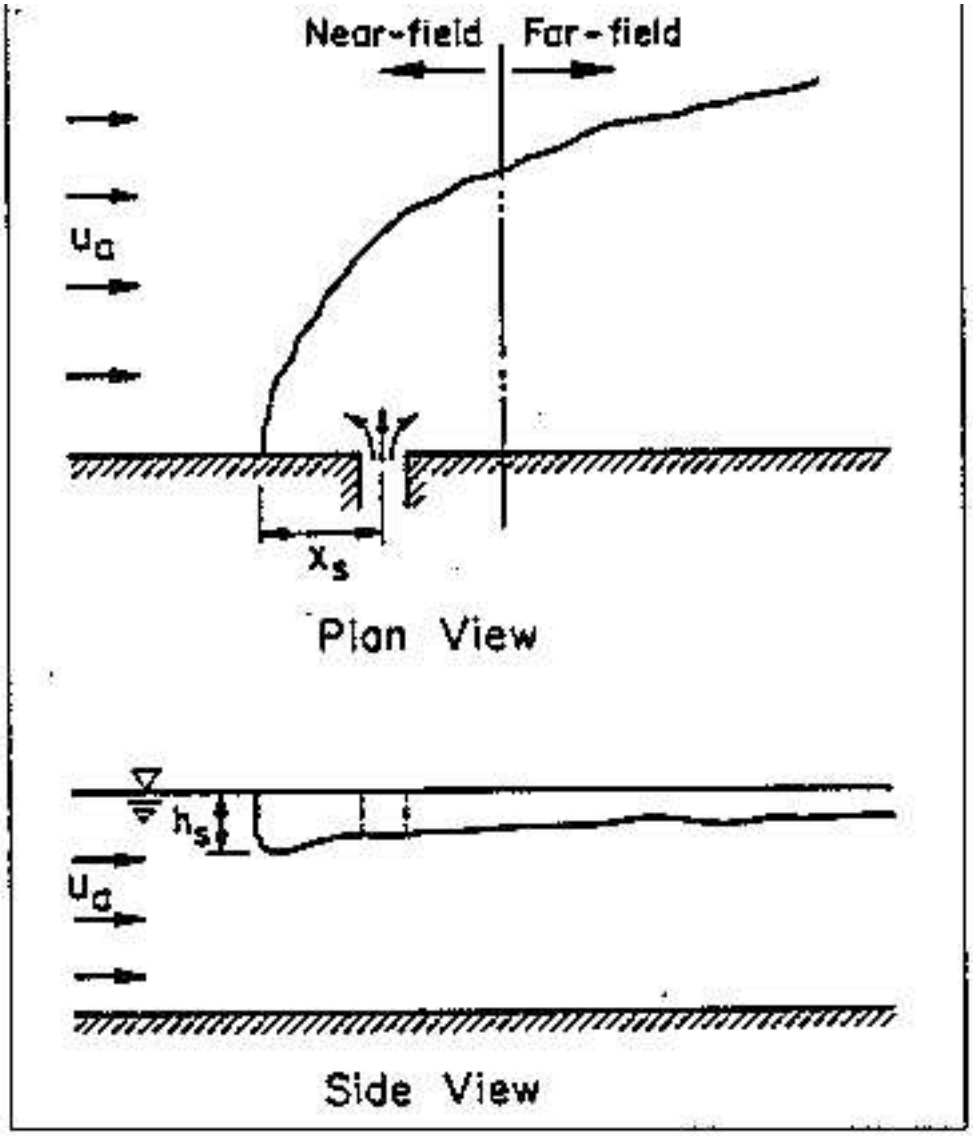

Figure 2.6a: Upstream intruding plume in a deep environment.

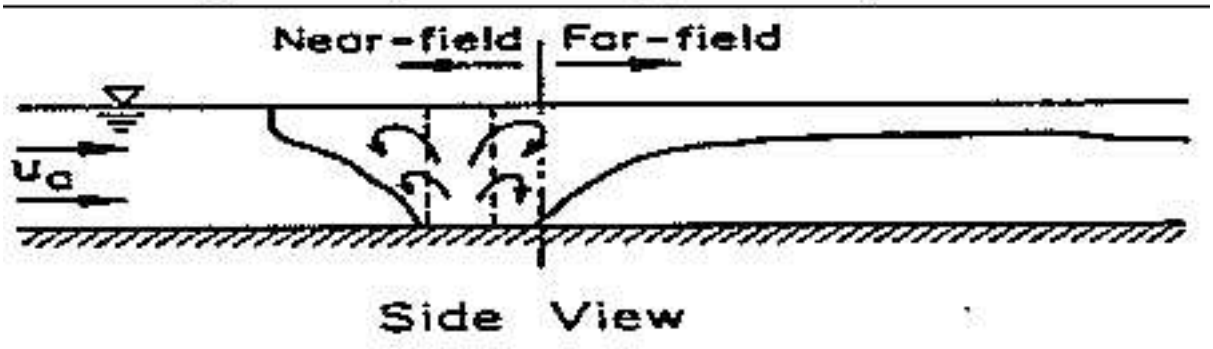

Fig 2.6b: Unstable upstream intruding plume in a shallow environment.

2.2.2. Jet-to-Plume Length Scale

The jet-to-plume length scale measures the relative importance of initial momentum and initial buoyancy. It is defined as:

$$L_Q = \frac{M_o^{3/4}}{J_o^{1/2}} \tag{2.2}$$

In the region where y << L_M momentum dominates the flow and therefore jet mixing prevails. Where y >> L_M, buoyancy dominates and strong lateral spreading prevails. For this reason, the jet-to-plume length scale is an important measure of where regimes characterized by jet mixing end and regimes characterized by buoyancy-induced lateral spreading begin (see Figure 2.7).

2.2.3. Jet-to-Crossflow Length Scale

The jet-to-crossflow length scale measures the relative significance of the initial momentum and the ambient crossflow velocity. It is defined as:

$$L_m = \frac{M_o^{1/2}}{u_a} \tag{2.3}$$

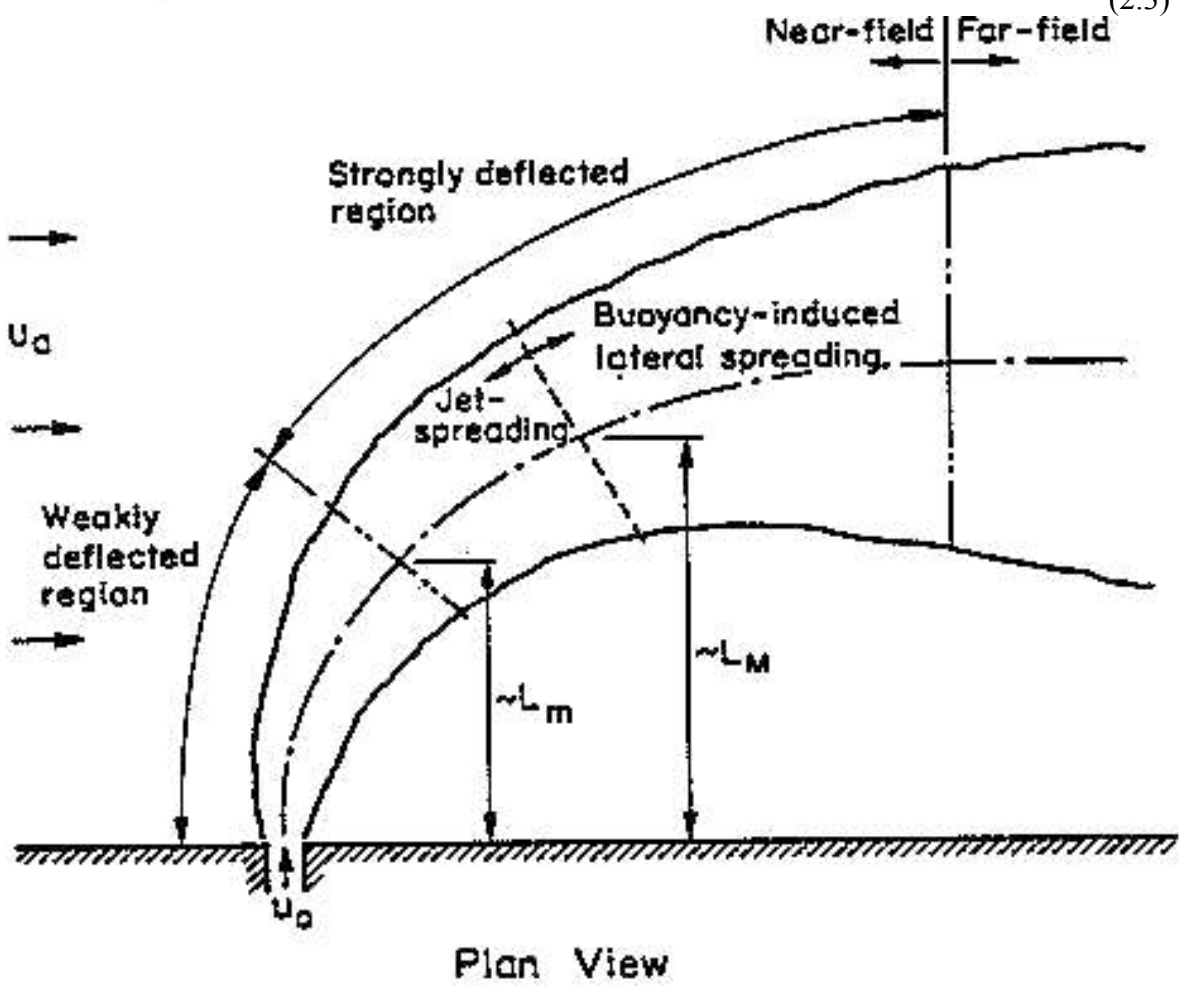

Figure 2.7: Example of length scale delineation of flow regimes for a free jet.

The jet-to-crossflow length scale is a measure of where the flow changes from the weakly deflected regime to the strongly deflected regime (see Figure 2.7).

2.2.4. Plume-to-Crossflow Length Scale

The plume-to-crossflow length scale measures the relative importance of the initial buoyancy flux to the ambient crossflow velocity. It is defined as:

$$L_b = \frac{J_o}{u_a^3} \tag{2.4}$$

The plume-to-crossflow length has a significantly different meaning for surface plumes than for submerged buoyant jets. Since this length scale represents an interaction of the initial buoyancy of the effluent and the velocity of the crossflow, its most apparent measure is the extent of upstream spreading that a surface plume may exhibit. It also plays a role in the increased lateral progression of free jets caused by the thinning of a buoyant surface jet due to buoyancy.

2.2.5. Two-dimensional Length Scales

When a flow is mixed over the entire water depth, it can be considered two-dimensional. In this case, all the flow parameters can be defined per unit depth. The appropriate flux definitions for two-dimensional situations are as follows:

$$q_o = Q_0 / H \tag{2.5}$$

$$m_o = M_o / H \tag{2.6}$$

$$j_0 = J_o / H \tag{2.7}$$

where H is the characteristic local ambient water depth. Using these two-dimensional fluxes, two-dimensional length scales can be defined as follows:

$$l_q = \frac{q_o^2}{m_o} \tag{2.8}$$

$$l_M = \frac{m_o}{j_o^{2/3}} \tag{2.9}$$

$$l_m = \frac{m_o}{u_a^2} \tag{2.10}$$

Note that a two-dimensional plume-to-crossflow length scale is not defined since it cannot exist on dimensional grounds (Akar, 1990).

2.2.6. Common Non-dimensional Numbers

Certain combinations of these length scales give some commonly used non-dimensional numbers, specifically the discharge densimetric Froude number, defined as:

$$Fr_{o'} = \frac{u_0}{\sqrt{g_{o'} a_o}^{1/2}} = L_M OVER L_Q \tag{2.11}$$

and the velocity ratio:

$$R = \frac{u_o}{u_a} = \frac{L_m}{L_Q} \tag{2.12}$$

Also, the quantity Fr_o'/R equals:

$$\frac{Fr_{o'}}{R} = \left(\frac{L_m}{L_b} \right)^{1/2} \tag{2.13}$$

which is an important factor in determining the trajectory of free jets as discussed in Section 2.3.3.3.

2.3. Near-field Flow Regime Analysis

The following sections provide the theoretical framework on which the analytical expressions used in the near-field flow regimes are based. These expressions are derived through the use of simple dimensional analysis which is discussed in Section 2.3.1. The subsequent section, Section 2.3.2, describes the mixing processes of surface buoyant jets discharging into a deep stagnant ambient environment. Sections 2.3.3 through 2.3.6 incorporate ambient crossflow and shallow water effects into the analysis of buoyant free jets, wall jets, shoreline-attached flows, and upstream intruding plumes respectively.

2.3.1. Dimensional Analysis of Surface Buoyant Surface Jets

The application of dimensional analysis to surface buoyant jets is based on two important assumptions. First, only fully turbulent flows are considered, and therefore the effects of viscosity can be neglected. Second, the Boussinesq approximation is assumed, that is, the density difference between the effluent and the ambient environment is small and is only important in terms of buoyancy forces.

The nine variables that effect the near-field flow of a surface buoyant jet are: the initial volume, momentum and buoyancy fluxes, Q_o, M_o, and J_o; the ambient velocity, u_a; the distance along the trajectory, s; the local ambient water depth, H; the width and depth of the discharge channel, b_o and h_o; and the discharge angle, Ã. Therefore any flow variable, Æ, can be described as a function of these independent variables:

$$\phi = f\left(Q_o, M_o, J_o, u_a, s, H, h_o, b_o, \sigma \right) \tag{2.14}$$

The independent variables may be manipulated into different dimensionless groups which may differ from regime to regime depending on which parameters are significant to the particular flow. Then the form of the solution for a particular regime is obtained by describing only the particular processes that dominate the flow in that regime and solving the simplified problem.

This is an asymptotic approach which provides solutions that are only valid within certain specified regimes and require experimentally determined coefficients. However, these solutions may be linked together so that appropriate expressions are used in succession providing an overall prediction for the entire problem.

The cartesian coordinate system used in this study is oriented with the origin at the mouth of the discharge, the x-axis pointing downstream, and the y-axis pointing across the current perpendicular to the ambient crossflow. This is illustrated in Figure 2.1.

2.3.2. Buoyant Surface Jet in a Stagnant Ambient Environment

A brief description of a free jet into a stagnant ambient environment is given in Section 2.1.1. As described in that section, the flow is comprised of two regimes: an initial regime of strong jet mixing with growth of the jet in both the vertical and horizontal directions, followed by a regime of increased buoyancy induced spreading for which the plume thickness decreases yet retains enough of the initial momentum to prevent the unstable buoyant pool which develops at the transition distance. This exemplified in Figure 2.3.

The transition between these two regimes is characterized by the jet-to-plume length scale L_M. As discussed in Section 2.2.2, the jet-to-plume length scale is a relative measure of the initial momentum and the initial buoyancy. For $y/L_M << O(1)$, the flow is dominated by the initial momentum and therefore is characterized by strong jet mixing. For $y/L_M >> O(1)$, the flow is dominated by the buoyancy and the lateral plume-like spreading becomes prevalent. In the case that $L_M << L_Q$ there will be no momentum dominated flow and the flow will be entirely plume-like.

In applying dimensional analysis to this problem, the ambient velocity u_a, depth parameter H, and the discharge angle Ã are neglected, therefore reducing Eqn. 2.14 to:

$$\phi = f\left(Q_o, M_o, J_o, s, h_o, b_o \right) \tag{2.15}$$

The non-dimensionalized form of the flow parameter, $Æ^*$, can then be described as a function of the following non-dimensional ratios:

$$\phi^* = f\left(\frac{s}{L_M}, \frac{L_Q}{L_M}, AR\right) \tag{2.16}$$

where AR is the discharge channel aspect ratio defined as h_o/b_o. Previous experience has indicated that the aspect ratio plays an insignificant role in flows with high local dilutions (Jirka et al., 1981).

2.3.2.1. Initial Jet-like Flow Characteristics

The initial regime, dominated by strong jet mixing, is analogous to one-half of a round submerged non-buoyant jet. After an initial zone of flow establishment (which will be neglected in the following analyses), the jet displays a full Gaussian velocity profile in the horizontal direction and a half Gaussian velocity profile in the vertical direction. Figure 2.8 demonstrates these profiles. The pollutant concentration exhibits similar Gaussian profiles. The centerline velocity, u_c, decreases with increasing distance along the centerline, s. However, total momentum flux, M, is conserved throughout this region. For jet-like flows with a Gaussian profile, the half-width b_h and vertical depth b_v of the flow are defined to be where the concentration is 1/e (37%) of the centerline concentration.

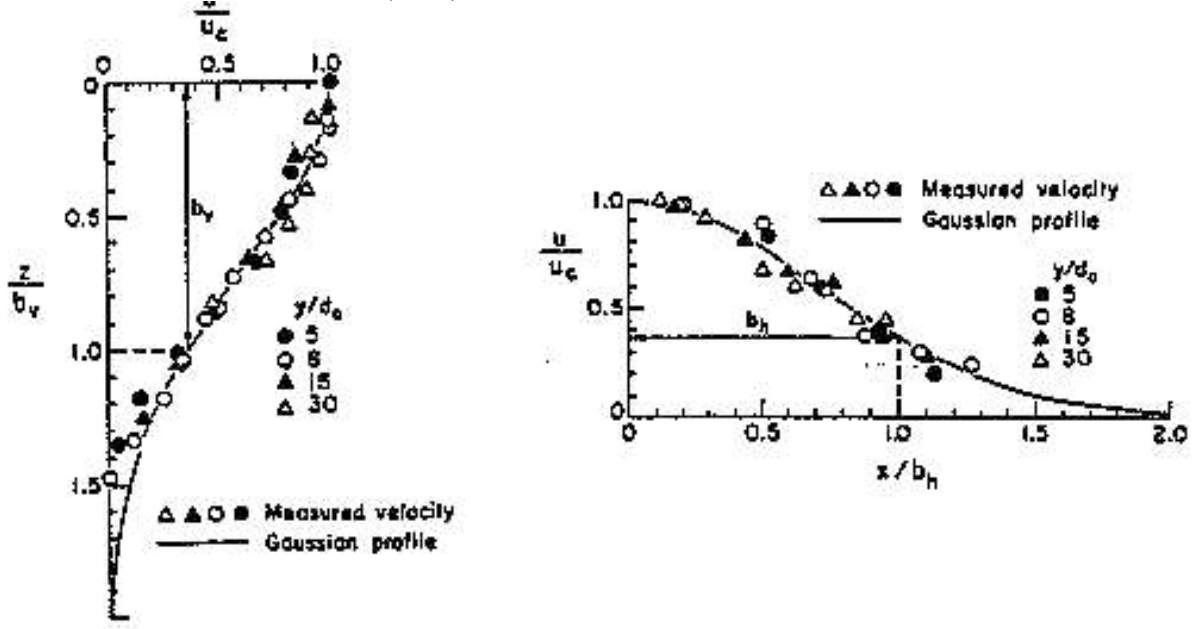

a) Vertical velocity profile. b) Horizontal velocity profile.

Fig 2.8: Guassian velocity profile of a non-bouyant surface jet (adapted from Rajaratam and Humphries, 1984)

From dimensional considerations, u_c is found to be a function of the initial momentum, M_o, and the distance along the trajectory centerline, s, as follows:

$$u_c = c_1 \frac{M_o^{1/2}}{s} \tag{2.17}$$

where c_1 is a constant. The only possible expression for the half-width that may be obtained from dimensional analysis is:

$$b = b_1 s \tag{2.18}$$

where b_1 is a constant. If the centerline dilution, S, is defined as C_o/C, where C_o is the initial discharge concentration and C is the centerline concentration, then the only dimensionally consistent relationship for S is:

$$S = s_1 \frac{M_o^{1/2}}{Q_o} s = s_1 \frac{s}{L_Q} \tag{2.19}$$

where s_1 is a constant. The constants c_1, b_1, and s_1 must be determined experimentally.

2.3.2.2. Jet-like Flow with Superimposed Buoyant Spreading

The following regime retains the initial momentum, therefore preserving the centerline velocity relationship given by Eqn. 2.17. However, the vertical bulk buoyant force acts on the flow that results in continuous deformation of the jet cross-section, increasing the horizontal spreading and vertical thinning. This buoyant spreading process can be considered a perturbation which may be superimposed on the jet-like centerline velocity (see Figure 2.3).

The buoyant spreading perturbation assumes the plume acts as a density current. Density currents generally entrain fluid in the frontal zones located at the edge of the plume, which spread laterally with a velocity v_B. Benjamin (1968) derived an equation for this spreading velocity:

$$v_B = \left(\frac{g' b_v}{C_D} \right)^{1/2} \tag{2.20}$$

C_D is the coefficient of drag for the flow and ranges from 0.5 to 2.0 (Doneker and Jirka, 1990). The density current is modelled as having a top-hat velocity profile. Therefore, the half-width b_h and depth b_v are defined at the edge of the flow as shown in Figure 2.9.

Along a streamline the spreading velocity can be written as $v_B = u_c(db_h/ds)$. Substituting this into Eqn. 2.20, we obtain:

$$\left(\frac{db_h}{ds}\right) = \frac{1}{u_c}\left(\frac{g' b_v}{C_D}\right)^{1/2} \tag{2.21}$$

Since buoyancy flux is conserved according to the identity $J_o = 2u_c g' b_v b_h$, the term g' in Eqn. 2.21 may be replaced by $J_o/(2u_c b_v b_h)$. If the centerline velocity relationship for a pure jet as given by Eqn. 2.17 is substituted in to Eqn. 2.21, the resulting expression is:

$$b_h^{1/2}\frac{db_h}{ds} = b_1 b_h^{1/2} + c_4 \left(\frac{1}{2C_D}\right)^{1/2} \frac{J_o^{1/2}}{M_o^{3/4}}\, s^{3/2} \tag{2.22}$$

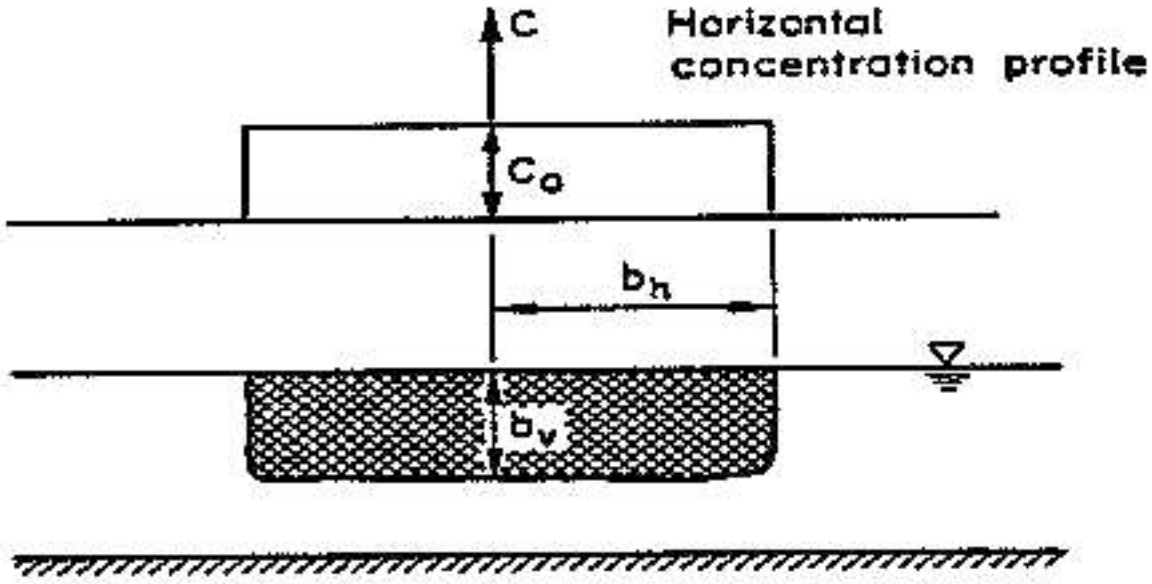

Fig 2.9 Cross-sectional voew og the top-hat concentration profile as defines for flows dominated by bouyant spreading.

A perturbation solution on basis of the non-buoyant behavior provides the final horizontal spreading relationship:

$$b_h = \left((b_1 s)^{3/2} + b_{b1} \left(\frac{1}{2C_D}\right)^{1/2} \frac{1}{L_M} (s - s_i)^{5/2} \right)^{2/3} \tag{2.23}$$

where b_{hi} and s_i are the initial half-width and distance along the trajectory at the beginning of this region and b_{b1} is a constant. Comparison to various laboratory results have proven this to be an accurate description of the buoyancy-induced spreading process.

Adapting the entrainment relationship $q_e(s) = \_v_B b_v$ where _ is a constant within the range 0.15 and 0.25 (Simpson and Britter, 1979; Jirka and Arita, 1987) and applying them as they are for far-field processes (Section 2.4.1), the vertical depth of the plume is obtained:

$$b_v = b_{vi} \left(\frac{b_h}{b_{hi}} \right)^{\beta-1} \tag{2.24}$$

If both buoyancy flux and pollutant flux are conserved, the ratio g'/g_o' can be used as an indicator of the dilution. As discussed in Section 2.4.1 for far-field processes, the dilution relationship is as follows:

$$S = S_i \left(\frac{b_h}{b_{hi}} \right)^{\beta} \tag{2.25}$$

where S_i is the initial dilution.

2.3.3. Free Jets in a Crossflow

By analogy to submerged buoyant jets, the trajectory of a buoyant free jet can be expected to pass through two phases (Jirka et al., 1981). The first is the weakly deflected region where the trajectory of the jet is similar to that of a pure momentum jet which is laterally deflected by the crossflow. In the second, the crossflow has bent the flow over and the jet/plume behaves like a line impulse which is gradually propagating perpendicular to the crossflow. Each of these regions are detailed in the following subsections 2.3.3.1 and 2.3.3.2.

The proper length scale to measure the transition between these two regions is the jet-to-crossflow length scale, L_m, discussed in Section 2.2.3. For $y/L_m << O(1)$, the crossflow is relatively unimportant and is treated as a small perturbation on the two regimes described in the stagnant case. This region is termed the "weakly deflected region." For $y/L >> O(1)$, the crossflow becomes the primary advecting mechanism for which alternate theories will be developed (Section 2.3.3.2) and is termed the "strongly deflected region."

Similar flow phases have been established for the trajectories of submerged jets. By comparing surface buoyant jet trajectory data with the expressions developed for submerged jets, Jirka et al. (1981) showed that it would be reasonable to use similar flow region delineation for surface buoyant jets. An updated version of this comparison has been duplicated in Figure 2.10. Note that there appears to be some systematic effect due to the ratio $Fr_o/R = (L_m/L_b)^{1/2}$. Correction for this effect is discussed in Section 2.3.3.3.

2.3.3.1. Weakly Deflected Flows

For a weakly deflected jet in a crossflow, the centerline velocity, half-width and dilution relationships developed for the initial jet-like mixing region in a stagnant environment (Eqns. 2.17, 2.18, and 2.19) still hold for this regime. However, the following perturbation is included to account for the downstream advection caused by the crossflow:

$$\frac{y}{L_m} = t_3 \left(\frac{x}{L_m} \right)^{1/2} \tag{2.26}$$

Substituting the centerline velocity given by Eqn. 2.17 into this expression and integrating gives the following trajectory relationship:

$$\frac{u_c}{u_a} = \frac{dy}{dx} \tag{2.27}$$

where t_1 is a constant which must be determined experimentally. This the same dependency found for the weakly deflected region of a submerged jet (Wright, 1977). It is also consistent with the dimensional analysis discussed in Section 2.3.1 and the data for the initial phase of surface buoyant jets shown in Figure 2.10.

For two dimensional flow, the same crossflow perturbation is applied as for the 3-dimensional case Eqn. 2.26, but the centerline velocity exhibits the following relationship (Holley and Jirka, 1986):

$$u_c = c_4 \left(\frac{m_o^{1/2}}{s^{1/2}} \right) \tag{2.28}$$

Substituting this centerline velocity definition into Eqn. 2.26 and integrating results in the following relationship:

$$\frac{y}{l_m} = t_4 \left(\frac{x}{l_m} \right)^{2/3} \tag{2.29}$$

The dilution is derived analogously to that of the 3-dimensional case but using the 2-dimensional flux and length scale definitions. This results in:

$$S = s_4 \left(\frac{y}{l_q} \right)^{1/2} \tag{2.30}$$

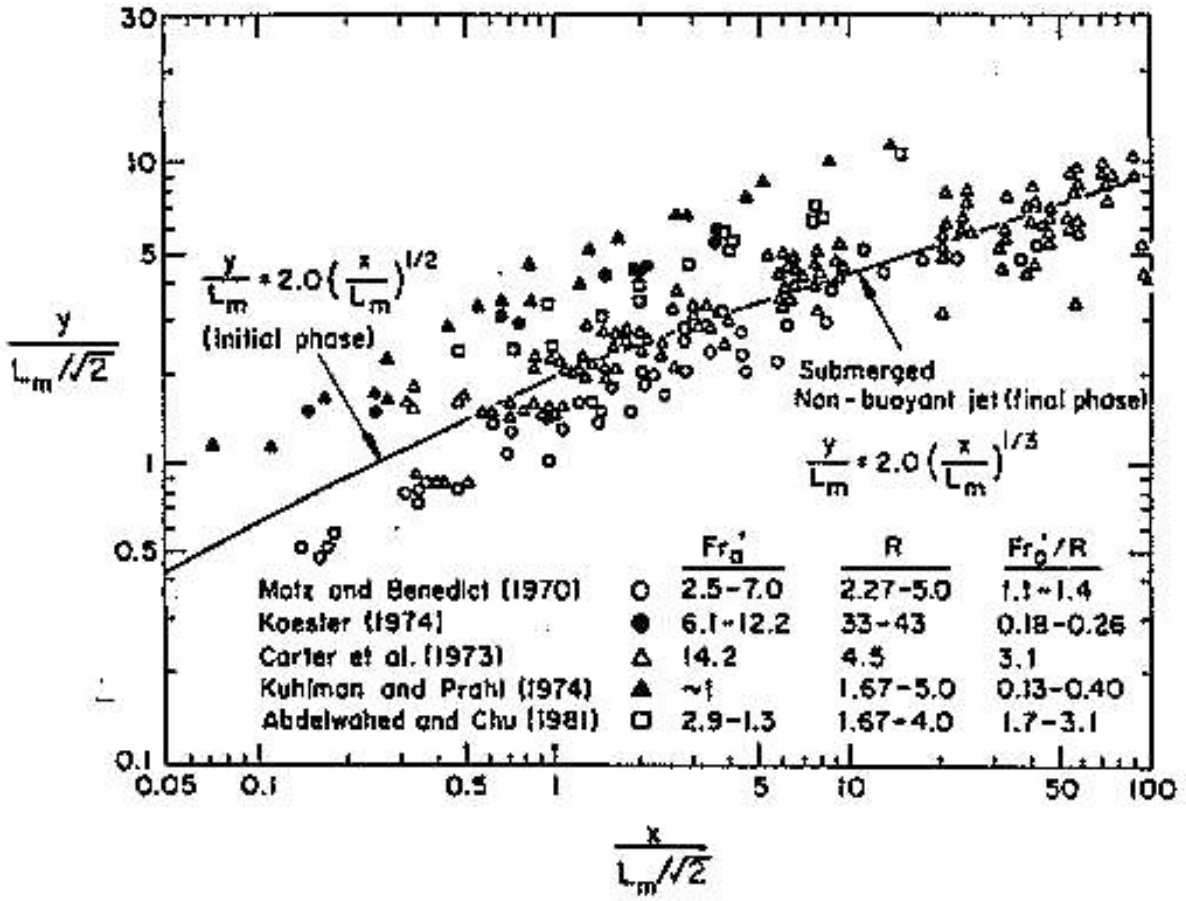

Fig 2.10: Trajectories of free jets in compatison to trajectory laws for submerged non-bouyant jets. (adapted from Chu and Jirka, 1986)

T
he horizontal half-width relationship is similar to Eqn. 2.18:

$$b = b_4\ y \tag{2.31}$$

but uses a different constant, b_4.

For cases where $L_M < L_m$, buoyancy induced spreading occurs in the weakly deflected region. In this case, the same trajectory relationship applies as for the weakly deflected jet (Eqn 2.27), but the half-width, depth and dilution relationships that apply are the same as for the buoyancy induced spreading in the second flow regime of the stagnant case, and are given by Eqns. 2.23, 2.24, and 2.25. This, in effect, superimposes the governing equations for a density current onto a flow whose trajectory is still momentum controlled.

2.3.3.2. Strongly Deflected Flows

In the strongly deflected region, where $y/L_m >> O(1)$, the flow is advected downstream with the ambient current at a velocity u_a. However, it still exhibits some lateral deflection due to some residual momentum force. This is modelled as an instantaneous release of non-buoyant fluid issued horizontally from a line source. This conceptualization, as described by Scorer (1959), can be described with appropriate dimensional analysis, where the significant variables are the line impulse M', the horizontal progression y, and the time after release t. The resulting expression is:

$$\frac{M't}{y^3} = const. \tag{2.32}$$

In applying this analogy to a pure jet, M' is replaced by M_o/u_a and t is replaced by y/u_a. This results in the following dimensionally consistent expression:

$$\frac{y}{L_m} = t_5 \left(\frac{x}{L_m}\right)^{1/3} \tag{2.33}$$

This is the same form as for a submerged non-buoyant jet which is strongly deflected and is consistent with the data shown in Figure 2.10. Again, the half-width relationship for a jet holds with a buoyant amplification factor, derived in a fashion similar to that leading to Eqn.2.23,

$$b = b_5\ y \left(1 + b_{b5} \frac{L_b^{1/2}}{L_m^{2}} (y - y_i)^{3/2} \right) \tag{2.34}$$

If we use the identity $C_oQ_o \propto C_cb_hb_vu_a$ to describe the mass conservation, then in terms of length scales the dilution $S = C_o/C_c$ is given by:

$$S = s_5 \left(\frac{y^2}{L_m L_Q}\right) \tag{2.35}$$

For 2-dimensional strongly deflected jets, a similar line impulse model is used resulting in the following relationship:

$$\frac{m't}{y^3} = const. \tag{2.36}$$

where m' is the line impulse per unit depth of discharge, m' = M'/H. Therefore, substituting m_o/u_a and y/u_a into Eqn. 2.36 as before, the following relationship is obtained:

$$\frac{y}{l_m} = t_6 \left(\frac{x}{l_m} \right)^{1/2} \tag{2.37}$$

The dilution is analogous to that of the 3-dimensional case but uses the 2-dimensional flux and length-scale definitions. The dilution for a strongly deflected 2-dimensional jet is then:

$$S = s_6 \frac{y}{(l_q l_m)^{1/2}} \tag{2.38}$$

The horizontal half-width equation is similar to Eqn. 2.18:

$$b = b_6 \; y \tag{2.39}$$

The above equations only apply for jet-like flows in the strongly deflected region, i.e.: when $L_m < y < L_M$. However, once buoyancy starts to deform the flow and buoyancy induced spreading becomes the dominate mixing process in this region, i.e.: when $y > L_m$ & L_M, the half-width and dilution expressions developed in Section 2.3.2.2 for buoyancy driven lateral spreading apply (Eqns. 2.23, 2.24, and 2.25). However, the trajectory relationship remains the same as developed for a strongly deflected jet (Eqn. 2.33).

2.3.3.3. Correction for Trajectory Constant

When buoyancy-induced spreading causes the plume to thin, the flow will tend to penetrate further into the crossflow. This can be seen by the systematic effect of Fr_o'/R on the trajectories of free jets in Figure 2.10. To estimate this trend of variability, run-averaged trajectory constants were plotted against Fr_o'/R as shown in Figure 2.11. A best-fit line was obtained using a regression that can be approximated by:

$$t = 2.0 \left(1 + 3.0 \exp - \left(\frac{\mathrm{Fr}_o'}{\mathrm{R}} \right)^2 \right) \tag{2.40}$$

The minimum trajectory constant was taken as 2.0, somewhat larger than the theoretical value for a non-buoyant wall jet (Holley and Jirka, 1986). The lower experimental values shown in Figure 2.10 are caused by boundary effects in narrow laboratory channels and are discounted for the purpose of Eqn.2.40.

2.3.4. Wall Jets

As noted in Section 2.1.1, wall jets are considered a special case of weakly deflected free jets. When the mirror image of a wall jet is considered, the flow is identical to that of a free jet issue in a coflow. Since the discharge is issued in a coflow, however, no strongly deflected region exists and any buoyancy induced spreading can be considered a far-field process.

Therefore, the two possible regimes that exist in the near-field of a wall jet are analogous to the 3-dimensional and 2-dimensional weakly deflected jet regimes. Using identical formulations as for the weakly deflected free jets but including a mirror image, the following dilution relationships are obtained for the 3-dimensional and 2-dimensional cases, respectively:

$$S = s_7 \left(\frac{x}{L_Q} \right) \tag{2.41}$$

$$S = s_8 \left(\frac{x}{l_q} \right)^{1/2} \tag{2.42}$$

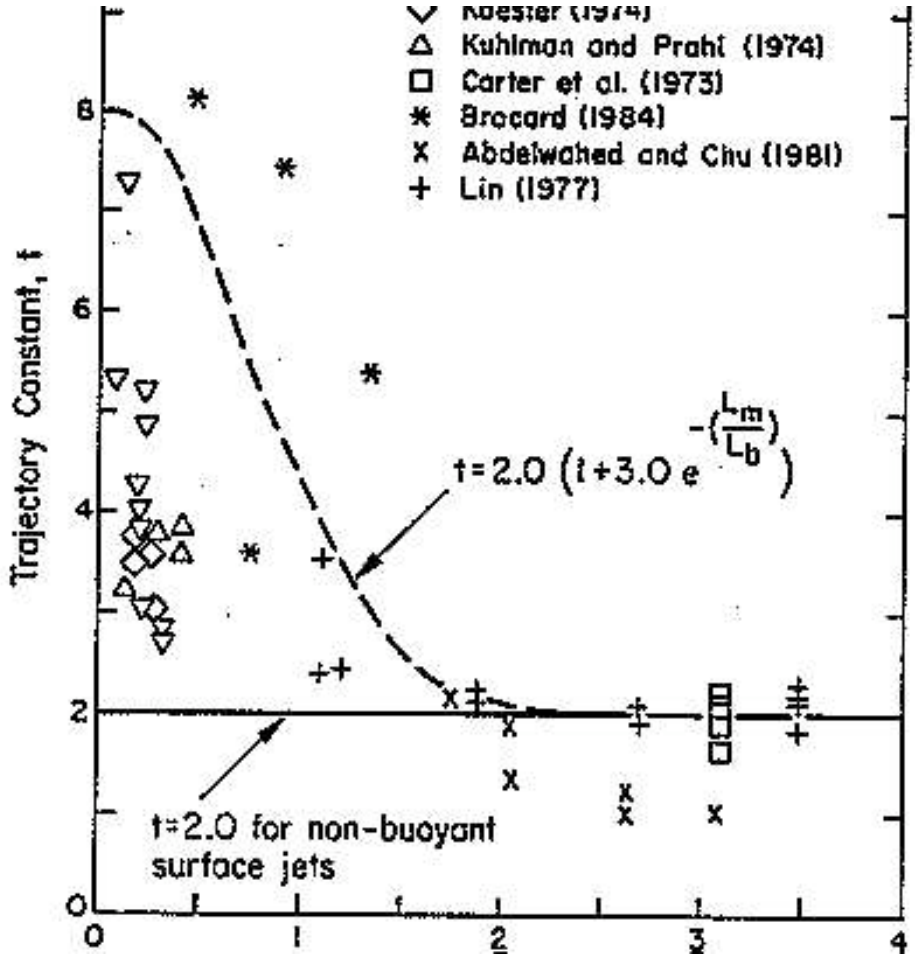

Fig 2.11: Variation of the tajectory constant with the ratio Fro'/R=(Lm/Lb)1/2.

where s_7 and s_8 are constants. The horizontal half-width retains a similar linear half-width relationship for both the 3-dimensional and 2-dimensional cases:

$$b_h = b_{7,8}\ x \tag{2.43}$$

where b_7 and b_8 are constants.

2.3.5. Shoreline Attached Flows

A qualitative description of shoreline attached flows is given in Section 2.1.2. Shoreline attached flows are typically strongly bent over with a recirculation region between the jet-like structure and the near bank. This is exhibited in Figure 2.5.

The bulk of the discharged fluid follows a trajectory similar to that of a free jet yet reduced in lateral penetration into the crossflow. Very often, the flow is strongly bent over very near the discharge so no weakly deflected region exists. Plots of shoreline attached flow trajectories show that the same power laws developed for free jets apply to shoreline attached flows as shown in Figure 2.12. Note, that the lateral progression is approximately half of that found for free jets. The lack of data for $y/L_m < 1$ is due to the fact that this weakly deflected region is typically very small and often negligible. As with free jets, there seems to be some systematic effect due to Fr_o'/R.

Since the trajectories of shoreline attached jets are analogous to free jets, similar trajectory relationships may be used for the 3-dimensional flows in the weakly deflected region and strongly deflected region, respectively:

$$\frac{y}{L_m} = t_9 \left(\frac{x}{L_m}\right)^{1/2} \tag{2.44}$$

$$\frac{y}{L_m} = t_{10} \left(\frac{x}{L_m}\right)^{1/3} \tag{2.45}$$

where t_9 and t_{10} are constants that are generally smaller than their free jet counterparts, depending on an attachment factor (see Chapter 4). For 2-dimensional jets, relationships similar to those for free jets also apply for the weakly deflected and strongly deflected regions, respectively:

$$(x, y) = (x', y') + (x_v, y_v) \tag{2.46}$$

$$\frac{y}{l_m} = t_{12} \left(\frac{x}{l_m}\right)^{1/2} \tag{2.47}$$

where t_{11} and t_{12} also depend on an attachment factor (see Chapter 5).

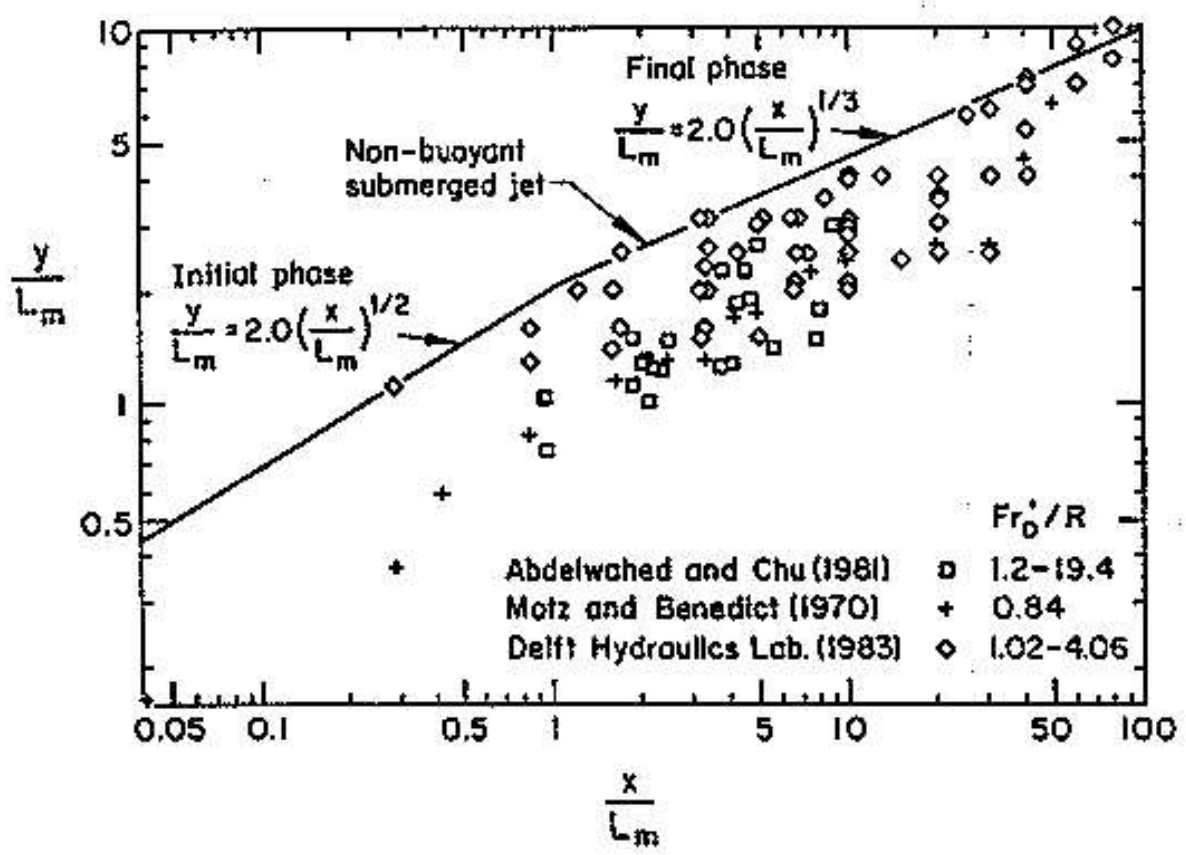

Fig 2.12: Trajectory data for the shoreline attached flows and comparison to submerges jet trajectory laws.

Similarly, the dilution and half-width relationships will be analogous to the free jet relationships. However, the dilution constants will be reduced due to the recirculation of the effluent along the downstream bank. The half-width definition only applies between the centerline and the outside edge of the flow since there is no definable half-width between the trajectory centerline and the near bank (see Figure 2.5).

2.3.6. Upstream Intruding Plumes

For very buoyant discharges into weak crossflows, the plume may spread upstream against the current. These upstream intruding plumes are qualitatively described in Section 2.1.3. The theoretical development of these plumes comes largely from studies by Jones et al. (1985) performed for radial surface and subsurface discharges.

Jones et al. define an intrusion length scale, L_I, which describes the interaction between the buoyant spreading force and the ambient crossflow.

$$L_I = \frac{J_o}{\pi C_{DI} U_a^3} = \frac{L_b}{\pi C_{DI}} \tag{2.48}$$

where C_{DI} is a drag coefficient on the order of unity (i.e.: O(1)).

Jones et al. provide a numerical solution for the upstream intrusion length, x_s, which can be approximated as follows:

$$\frac{x_s}{L_I} = 3.77 \left(\frac{L_M}{L_I} \right)^{2/3} \qquad for \ \frac{L_M}{L_I} \geq 0.356 \tag{2.49}$$

$$\frac{x_s}{L_I} = 1.9 \qquad for \ \frac{L_M}{L_I} < 0.356 \tag{2.50}$$

Jones et al. also developed a relationship for the bulk dilution at the end of the "intermediate region" which is approximately located at $x_f = x_s$. The relationship is approximated as:

$$S_f = \frac{0.81}{(\pi C_{D1})^{1/3}} L_M^{2/3} OVER L_Q \, L_b^{1/3} \tag{2.51}$$

Jones et al. give the typical depth of flow in the upstream intrusion region, h_s, as:

$$h_s = \frac{C_{D2} \ u_a^2}{g'} \tag{2.52}$$

where $C_{D2} \approx 0.8$. Since buoyancy flux is conserved, $g' = g_o'/S$. Therefore, using the above definition of dilution and writing Eqn. 2.51 in terms of length scales, h_s is equivalent to:

$$h_s = \left(\frac{0.405 \ C_{D2}}{(\pi C_{D1})^{1/3}} \right) \frac{L_M \ L_Q}{L_m} \tag{2.53}$$

The width of the plume b_h at the source is predicted as approximately 2.6 times the length of the upstream intrusion length. The width of the plume at the end of the near-field region is estimated as approximately $4.0x_s$.

$$b_{h,x=0} = 2.6 \ x_s \tag{2.54}$$

$$b_{hf} = 4.0 \ x_s \tag{2.55}$$

By continuity, the vertical depth of the plume at the end of this region can be computed as:

$$b_{vf} = \frac{S_f \; L_m \; L_Q}{b_{hf}} \tag{2.56}$$

If the depth at the discharge is shallow and the effluent is discharged with reasonably high momentum and buoyancy, the flow may be unstable and full vertical mixing may occur as shown in Figure 2.6b. Because of recirculation, dilutions are reduced. From dimensional analysis, the dilution of this flow pattern can be concluded to be in the following form:

$$S = s_{13} \frac{H_D^{5/3}}{L_M^{2/3} L_Q} \tag{2.57}$$

where s_{13} must be determined experimentally..

Restratification will generally occur in this plume-like flow just downstream of the point of discharge. The point of restratification will be used for the end of this regime and the beginning of the far-field. Restratification of the flow occurs at a distance approximately $H_D$downstream of the discharge (Doneker and Jirka, 1990), therefore $x_f = H_D$. The same half-width, depth, and upstream intrusion length as used for the stable case apply to this unstable regime.

2.4. Far-field Flow Regime Analysis

Two processes which occur in the far field are buoyant spreading followed by passive diffusion. buoyant spreading may or may not occur depending on the buoyancy and hydrodynamics of the flow, all discharges, if taken far enough downstream, are affected by ambient turbulence and therefore become passively diffused. The following two subsections (Sections 2.4.1 and 2.4.2) describe the theoretical development of these two processes; however, for more detail, the reader is referred to Akar and Jirka (1994a,b).

2.4.1. Buoyant Spreading Process

For strongly buoyant discharges, the far-field may exhibit strong lateral spreading and vertical thinning. This is similar to the buoyancy-driven spreading process described in Section 2.3.2.2 for the near-field. However, in the far-field there is no net lateral movement of the plume and the plume is advected downstream with the ambient current at a velocity u_a.

The definition diagram and structure of a surface buoyant spreading process in unstratified crossflow is shown in Figure 2.13. The laterally spreading flow behaves like a density current and entrains ambient fluid in the "head region" of the current. The mixing rate is usually relatively small. Furthermore, the flow may interact with a nearby bank or shoreline. The flow depth may decrease during this phase. The analysis of this region is analogous to the arguments presented in Section 2.3.2.2 for buoyancy-induced spreading in the near-field.

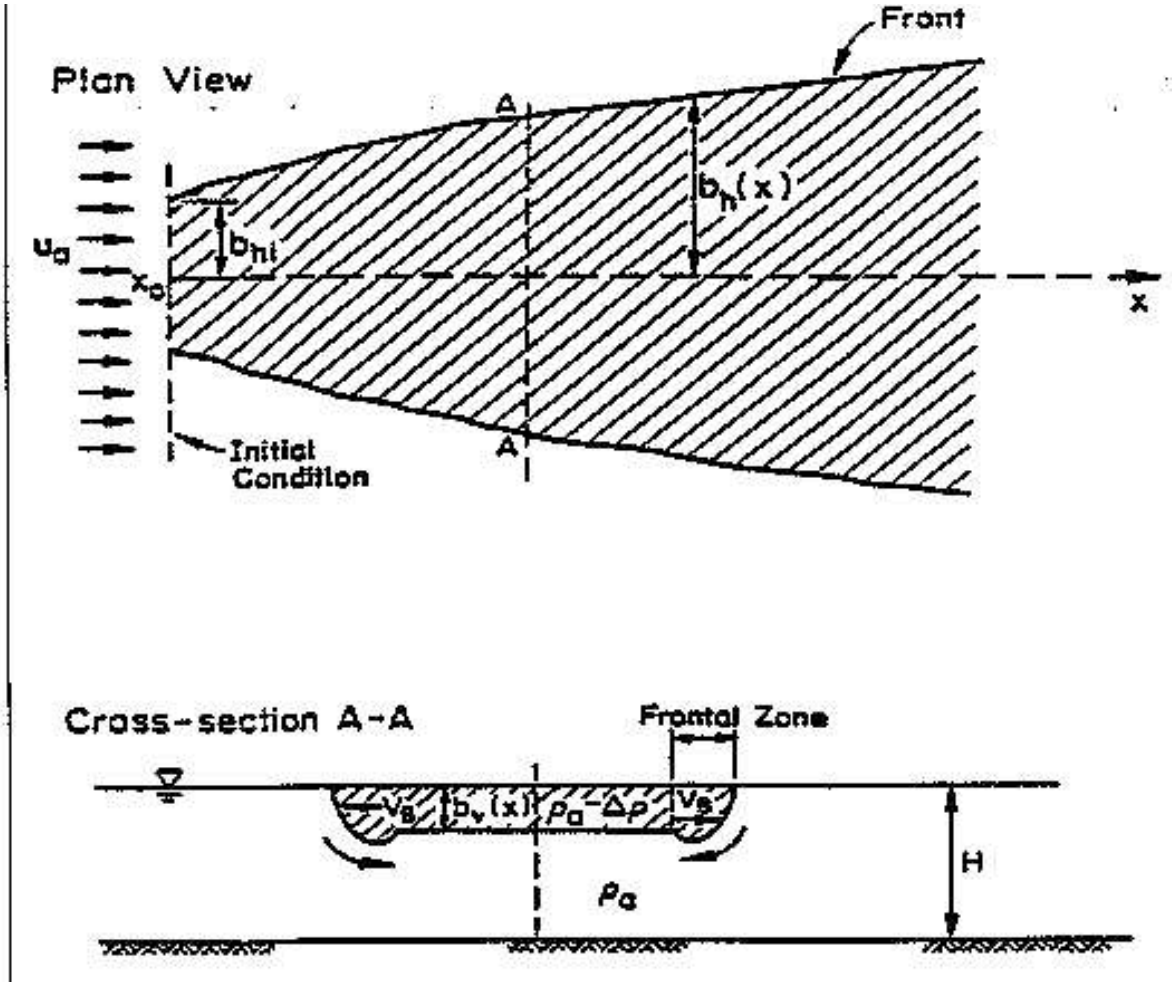

Fig 2.13: Bouyant surface spreading proces (from Doneker and Jirka, 1990)

The continuity equation for the density current is:

$$u_a \frac{\partial b_v}{\partial x} + \frac{\partial (v b_v)}{\partial y} = w_e \qquad (2.58)$$

where w_e is the net velocity across the interface and v(x,y) is the local transverse velocity. Combining the equation for the spreading velocity v_B developed by Benjamin (Eqn.2.20) with Eqn. 2.58 and integrating laterally over the density current half-width gives:

$$u_a \frac{d(b_h b_v)}{dx} = q_e(x) \qquad (2.59)$$

where $q_e(x)$ is the localized head entrainment representative of the dominant mixing mechanism.

The localized head entrainment of the density current is parameterized as $q_e(x) = ß v_B b_v$ where ß is a constant with a range of 0.15 to 0.25 (Simpson and Bitter, 1979; Jirka and Arita, 1987).

The flow half-width b_h is obtained for any downstream distance x by using the boundary condition for the streamline ($v_B = u_a db_h/dx$) and integrating Eqn. 2.58.

$$b_h = \left[b_{hi}^{3/2} + \frac{3}{2}\left(\frac{L_b}{2C_D}\right)^{1/2} (x - x_i) \right]^{2/3} \tag{2.60}$$

where x_i is the downstream distance at the beginning of the buoyant spreading region, and b_{hi} is the initial density current half-width. C_D is the coefficient of drag for the head region of the flow and ranges from 0.5 to 2.0 (Doneker and Jirka, 1990). This 2/3 power law of flow spreading is in agreement with the previous work of Larsen and Sorensen (1968).

The vertical flow half-width b_v is given by integrating Eqn. 2.59 to obtain:

$$b_v = b_{vi}\left(\frac{b_h}{b_{hi}}\right)^{\beta-1} \tag{2.61}$$

Due to mixing in the head region, the local concentration C and local buoyancy g' gradually change with distance x. The bulk dilution S, given by C_0/C, is equivalent to the ratio g_0'/g'. Since buoyancy flux is conserved, the identity $u_a g' b_v b_h$ = constant may be combined with the initial conditions to obtain the following expression for dilution:

$$S = S_i\left(\frac{b_h}{b_{hi}}\right)^{\beta} \tag{2.62}$$

where S_i is the initial dilution.

2.4.2. Passive Ambient Diffusion

The existing turbulence in the ambient environment becomes the dominating mixing mechanism at sufficiently large distances from the discharge point. In general, the passively diffusing flow is growing in width and in thickness (see Figure 2.14). Furthermore, it may interact with the channel bottom and/or banks.

The analysis of this region follows classical diffusion theory (e.g.: Fischer et al., 1979). The standard deviation σ_s of a diffusing plume in crossflow can be written in terms of the transverse turbulent diffusivity E:

$$\sigma_s^2 = \frac{2E_x}{u_a} \tag{2.63}$$

in which x is the distance following the ambient flow with the point release located at x = 0. The coefficient of eddy diffusivity depends on the turbulence conditions in the environment and may be a function of distance x (or plume size σ_s).

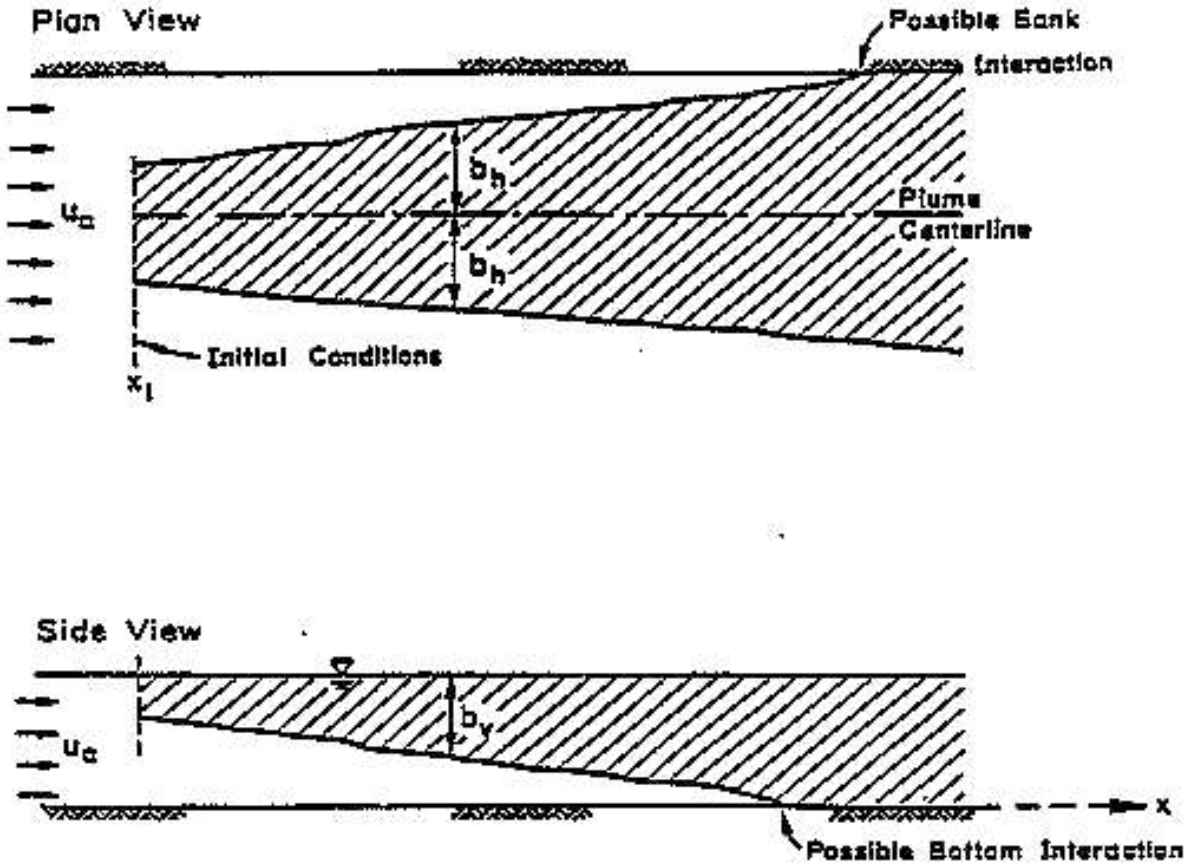

Fig 2.14: Passive ambient diffusion process (from Doneker and Jirka, 1990)

2.4.2.1. Diffusion in Bounded Channel Flow

In open channel flow the eddy diffusivity can be related to the friction velocity u_* and the channel depth H

$$E_z = 0.2 u_* H \tag{2.64}$$

for vertical diffusivity, and

$$E_y = 0.6 u_* H \tag{2.65}$$

for horizontal diffusivity. The friction velocity is given by $u_* = (f/8)^{1/2} u_a$ where f is the Darcy-Weisbach friction factor. Due to some anisotropy in a typical channel flow, the diffusivity in the horizontal transverse direction is usually larger than the diffusivity in the vertical direction. The coefficients included in Eqns. 2.64 and 2.65 are average values for reasonably uniform channels. The coefficients may be considerably larger (up to a factor of 2) for highly non-uniform cross-sections and/or strongly curved channels (see also Holley and Jirka, 1986).

Solution of Eqn. 2.63 with these diffusivities and with initial flow half-width conditions specified at x_i (see Figure 2.14) gives the vertical thickness b_v and half-width b_h, respectively:

$$b_v = \left[\frac{\pi E_z (x - x_i)}{u_a} + b_{vi}^2 \right]^{1/2} \tag{2.66}$$

$$b_h = \left[\frac{\pi E_y (x\ x_i)}{u_a} + b_{hi}^2 \right]^{1/2} \tag{2.67}$$

where x_i, b_{vi}, and b_{hi} are the distance, half-width, and depth of the plume at the beginning of the passive diffusion region. The above definitions are related to the vertical and horizontal standard deviations by a factor of $(\pi/2)^{1/2}$: $b_v = (\pi/2)^{1/2}\pi_{sv}$ and $b_h = (\pi/2)^{1/2}\tilde{A}_{sh}$, assuming an equivalent top-hat plume with same centerline concentration and pollutant mass flux.

Applying the continuity equation $2u_a b_v b_h \approx SQ_o$ yields the dilution:

$$S = \frac{2 b_v b_h}{L_m\ L_Q} \tag{2.68}$$

Beyond the distance at which the flow becomes fully mixed (b_v = H), the dilution expression is:

$$S = \frac{2 H b_h}{L_m\ L_Q} \tag{2.69}$$

2.4.2.2. Horizontal Diffusion in Unbounded Channel Flow

Many environmental flows without any significant limitation on the transverse dimension (coastal water, large lakes, etc.) exhibit an accelerating turbulent diffusive growth pattern. The horizontal diffusivity is often specified by the so called "4/3 law" (see Fischer et al., 1979):

$$E_y = \alpha (3\ \sigma_{sh})^{4/3} \tag{2.70}$$

in which ± is a coefficient equal to 0.01 $cm^{2/3}/s$ (appropriate for small plume sizes) and E_y is in units of [cm^2/s] and $\tilde{A}_{sh}$ in [cm]. Integration of the applicable diffusion equation with this variable E_y yields a solution for plume growth (Brooks, 1960, and Fischer et al., 1979):

$$b_h = b_{hi}\left[1 + \left(\frac{\pi}{3}\right)\frac{E_{yi}(x - xSUBi)}{u_a\ b_{hi}^2}\right]^{3/2} \tag{2.71}$$

using the present notation and half-width convention. E_{yi} is the initial value of diffusivity, so from Eqn. 2.70 at position x_i:

$$E_{yi} = 0.0015\ b_{hi}^{4/3} \tag{2.72}$$

with units of [m^2/s] for E_{yi} and [m] for the initial half-width b_{hi}. The dilution expressions are the same as before, given by Eqns. 2.68 and 2.69.